# EFFECTS OF BORON COMPOUND ON CHARACTERISTICS OF POLY(METHYL METHACRYLATE) AND ITS NANOCOMPOSITES

A THESIS SUBMITTED TO
THE GRADUATE SCHOOL OF NATURAL AND APPLIED SCIENCES
OF
MIDDLE EAST TECHNICAL UNIVERSITY

BY

MÜBERRA GÖKTAŞ

IN PARTIAL FULFILLMENT OF THE REQUIREMENTS
FOR
THE DEGREE OF MASTER OF SCIENCE
IN
POLYMER SCIENCE AND TECHNOLOGY

JUNE 2016

Approval of the thesis:

**EFFECTS OF BORON COMPOUND ON CHARACTERISTICS OF POLY(METHYL METHACRYLATE) AND ITS NANOCOMPOSITES**

submitted by **MÜBERRA GÖKTAŞ** in partial fulfillment of the requirements for the degree of **Master of Science in Polymer Science and Technology Department**, **Middle East Technical University** by,

Prof. Dr. Gülbin Dural Ünver _____
Dean, Graduate School of **Natural and Applied Sciences**

Prof. Dr. Necati Özkan _____
Head of Department, **Polymer Science and Technology**

Prof. Dr. Jale Hacaloğlu _____
Supervisor, **Chemistry Department, METU**

Prof. Dr. Ayşen Yılmaz _____
Co-supervisor, **Chemistry Department, METU**

**Examining Committee Members:**

Prof. Dr. Necati Özkan _____
Polymer Science and Technology, METU

Prof. Dr. Jale Hacaloğlu _____
Chemistry Department, METU

Assoc. Prof. Dr. İrem Erel Göktepe _____
Chemistry Department, METU

Prof. Dr. Cevdet Kaynak _____
Metallurgical and Materials Engineering, METU

Prof. Dr. Zeki Öktem _____
Chemistry Department, Kırıkkale University

**Date:** 07.06.2016

**I hereby declare that all information in this document has been obtained and presented in accordance with academic rules and ethical conduct. I also declare that, as required by these rules and conduct, I have fully cited and referenced all material and results that are not original to this work.**

Name, Last name: MÜBERRA GÖKTAŞ

Signature:

# ABSTRACT

## EFFECTS OF BORON COMPOUND ON CHARACTERISTICS OF POLY(METHYL METHACRYLATE) AND ITS NANOCOMPOSITES

Göktaş, Müberra

M.S., Polymer Science and Technology Department

Supervisor: Prof. Dr. Jale Hacaloğlu

Co-Supervisor: Prof. Dr. Ayşen Yılmaz

June 2016, 86 Pages

In this work, composites of poly(methyl methacrylate) and benzene-1,4-diboronic acid (BDBA) and their nanocomposites with organically modified montmorillonite OMMT prepared by solution and melt mixing, were characterized to study effects of boron content and the preparation method on the properties of PMMA.

SEM images showed homogeneous dispersion of BDBA particles for the melt blended, whereas, agglomeration for the solution mixed PMMA/BDBA composites. XRD and TEM results of PMMA nanocomposites indicated that its nanocomposites prepared by both techniques were generally consisted of intercalated/exfoliated OMMT layers.

Thermogravimetric analysis (TGA) and direct pyrolysis mass spectrometry (DP-MS) indicated an increase in the thermal stability of the composites upon incorporation of boron and Cloisite 30B into PMMA matrix prepared by both techniques. This behavior was associated with generation of units by trans-esterification reactions between BDBA and PMMA. In addition, at high BDBA loadings, formation of a boron network structure was recorded for the composites prepared by solution casting technique. During the degradation of the PMMA nanocomposites with OMMT, the interactions between BDBA and ester groups of PMMA became more dominant than those among BDBA particles generating a boron network structure.

Limiting oxygen index (LOI) and UL-94 vertical tests revealed no significant improvement in flammability characteristics for the composites. In addition, noticeable decrease in % elongation at break and tensile strength of PMMA was observed although stiffness of the polymer was slightly improved upon addition of BDBA and organoclay.

**Keywords:** Poly(methyl methacrylate) (PMMA), Boron Compound, Benzene-1,4-Diboronic acid, Organically Modified Montmorillonite, Thermal Characterization, Direct Pyrolysis Mass Spectrometry

# ÖZ

## BORON BİLEŞİĞİNİN POLİ (METİL METAKRİLAT) VE NANOKOMPOZİTLERİNİN ÖZELLİKLERİNE ETKİLERİ

Göktaş, Müberra

Yüksek Lisans, Polimer Bilimi ve Teknolojisi Bölümü

Tez Yöneticisi: Prof. Dr. Jale Hacaloğlu

Yardımcı Tez Yöneticisi: Prof. Dr. Ayşen Yılmaz

Haziran 2016, 86 Sayfa

Bu çalışmada; poli(metil metakrilat), (PMMA) ve benzen-1,4-diboronik asit, (BDBA) içeren eriyik ve çözelti karıştırma yöntemleri ile hazırlanmış kompozitleri ve bunların organik olarak modifiye edilmiş montmorillonit ile nanokompozitleri, boron varlığının ve hazırlama yöntemlerinin PMMA özelliklerine etkilerini belirlemek amacıyla karakterize edildi.

SEM fotoğrafları eriterek hazırlanan kompozitlerde BDBA parçalarının homojen olarak dağıldığını gösterirken, çözerek hazırlanan kompozitlerde topaklanmış alanların oluştuğunu gösterdi. PMMA nanokompozitlerinin XRD ve TEM sonuçlarında ise, her iki yöntemle de hazırlanmış nanokompozitlerin

genellikle birbirinden uzaklaşmış ve polimer matris içerisinde dağılmış kil tabakalarından oluştuğu tespit edildi. .

Termogravimetrik analiz (TGA) ve doğrudan piroliz spektrometre (DP-MS) ile boron ve OMMT'nin PMMA matrisine eklenmesi, polimerin termal kararlılığını artırdığını göstermiştir. Bu davranış BDBA ve PMMA arasında karşılıklı esterleşme reaksiyonu sonucunda oluşan yapılardan kaynaklanmaktadır. Ayrıca, çözerek hazırlanan yüksek miktarda BDBA içeren kompozitlerde, boron ağ yapısının oluşumu tespit edildi. Termal kararlılığı OMMT ilavesi ile artan PMMA nanokompozitlerinin termal bozunumu sırasında, BDBA ve PMMA'nın ester grupları arasındaki etkileşim boron ağ yapısına neden olan BDBA partiküllerinin kendi aralarındaki etkileşimden daha baskın olmuştur.

LOI ve UL-94 yanmazlık testlerinde, eklenmiş olan katkı maddelerin polimer malzemeye alev geciktirici etkisi gözlenmedi. Ek olarak, kopma anına kadar ki uzama miktarlarının ve çekme dayanımlarının katkı maddeler ile azaldığı, malzemelerin tokluğunda ise az bir miktarda artma olduğu çekme testi ile gözlemlendi.

**Anahtar Kelimeler:** Poli (metil metakrilat) (PMMA), Bor Bileşiği, Benzen-1,4-Diboronik Asit, Montmorillonit, Termal Karakterizasyon, Doğrudan Piroliz Kütle Spektrometresi

***to my family...***

## ACKNOWLEDGEMENTS

I would like to express my sincere appreciation to my supervisor Prof. Dr. Jale Hacaloğlu for her endless supports, understanding, valuable advices, and encouragement during my study. She always helped me to improve my point of view and criticism and all the time she advised me to overcome my weakness with her credible knowledge and kind attitude. She is one of the most honest and compassionate person I have ever known and therefore I feel very lucky to study in her laboratory.

I am very thankful to Ümit Tayfun for spending a lot of his time to help my studies especially in the preparation of composites. Also, I am a lot indebted to Prof. Dr. Erdal Bayramlı for giving me permission of using the equipment in his laboratory. Moreover, Tuğba Kaya Deniz assisted me in a lot of issues and I am very grateful for her supports.

I would like to offer my thanks to Prof. Dr. Ayşen Yılmaz and her research group because of their helps and of giving me opportunity of using XRD instrument in any time.

Also, I am grateful to Yeliz Akpınar in order to supply relevant equipment for TEM analysis and to give a lot of important advices which made my works much easier.

I want to offer special thanks to my laboratory mates, Alinda Öykü Akar, Esra Özdemir, Nehir Utku, Ayşegül Hisar Telli and Halil İpek for their endless supports and kindly advices. During this period, my dear friends Emre Çubukcu, Fatih Şahin, Merve Özdemir, Büşra Rakop and the beloved people in METU Turkish Folklore Club always supported me and I am very lucky to have friends like you.

Finally, I would like to thank to my father, mother, sisters and specially my sister’s little child Ahmet Yağız for loves and making me happy. Their encouragements and supports have not come to an end and this gives me energy during my study.

## TABLE OF CONTENTS

# LIST OF FIGURES

## FIGURES

# LIST OF SCHEMES

## SCHEMES

# LIST OF TABLES

## TABLES

## LIST OF ABBREVIATIONS

| | |
|---|---|
| **AIBN** | Azobisisobutyronitrile |
| **BDBA** | Benzene-1,4- diboronic acid |
| **BN** | Boron nitride |
| **C30B** | Cloisite 30B |
| **HIPS** | High impact polystyrene |
| **LDPE** | Low density polyethylene |
| **MMA** | Methyl methacrylate |
| **MMT** | Montmorillonite |
| **PMMA** | Poly(methyl methacrylate) |
| **PO** | Polyolefin |
| **PPE** | Poly(phenyl ether) |
| **PVB** | Poly(vinyl borate) |
| **PVC** | Poly(vinyl chloride) |
| **OMMT** | Organically modified montmorillonite |
| $\mathbf{T_g}$ | Glass transition temperature |
| **TIC** | Total ion current |

# CHAPTER 1

# INTRODUCTION

Polymeric materials have been widely used in industry and daily life due to their significant properties such as low weight, high strength, ease of processing especially in producing products with complex shape and lower raw material costs. Because of these features, polymeric materials have taken the place of traditional materials like wood and metals for some applications. However, the characteristic properties of the polymers are not sufficient alone for many engineering applications which in many cases can be accomplished by the addition of fillers that means producing composite materials. Combining the fillers and polymers can display improvements in different properties. For example, addition of the fiber reinforcement to the polymer matrix can lead to enhanced mechanical properties. Rubbers can be used to increase impact strength, some particle reinforcements are used as flame retardant and by adding some conductive fillers, conductivity of the polymer can be improved drastically.

The advantage of the composite material is light weight product with intrinsic properties which are important for many industrial applications such as transportation vehicles, ballistic protection, sporting goods, musical instrument etc. However, they have some disadvantages such as being more brittle materials than metals, having high raw material and high fabrication cost especially for fiber reinforced composite materials.

When thermoplastics are subjected to high temperature, they thermally decompose and produce volatile gases, solid carbonaceous char and smoke. As mentioned before, some particles are used to improve thermal properties of the polymers. For example, halogen, phosphorus, nitrogen, silicon, and boron containing flame retardants and miscellaneous inorganic additives can be used as flame retardants for polymers. Halogen containing compounds are producing toxic gases and corrosive combustion product during burning even if they cause high level of enhancements in flame retardancy. The new trend in flame retardancy is to use halogen free flame retardant materials such as boron compounds and phosphorous. Boron compounds have an effective role in the condensed phase by producing char during burning. They produce a char layer on the polymer surface and hence block the oxygen interaction with the surface and also slow the motion of volatile gases away from the material. Boric acid and sodium borate (borax) are used as fire retardant primarily for cellulosic materials. They have an active role in dehydration and char formation with the oxygen containing substrates. Another boron compound mostly used in PVC, polyolefin, elastomer, polyamides and epoxy resins is zinc borate.

On the other hand, fillers in nanoscale dimension have gained importance in enhancement of the mechanical, thermal, electrical and barrier properties of the polymer matrix compared to the same volume fraction of micro particles. Besides all these advantages, fillers can affect the rheological properties of the polymers which lead to difficulties during processing of molten state. Therefore, polymer nanocomposites have been a field of growing research study in academic and industrial world during the last decade.

## 1.1. Nanoparticles

According to dimension, three types of nanofillers are classified as 3D,2D, 1D and 0D as shown in Figure 1.1. These numbers specify the number of dimensions which are not in the nanoscale size. The first kind of nanofillers is in the form of

three dimensional framework structures such as zeolites. The second class involves the layered structures with thickness smaller than 100 nm. These are in the form of plates, laminas and shells such as layered silicates which are called nanoclay. One dimensional fillers consist of nanofibers, nanotubes, nanorods such as carbon nanotubes. Finally, nanoparticles such as metal oxides and their clusters are named as zero dimensional nanofiller [1].

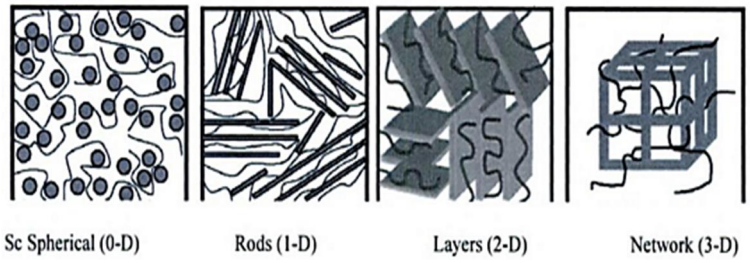


**Figure 1.1.** Classification of nanofillers according to their nano-dimensions [1]

### 1.1.1. Montmorillonite (MMT)

Clay was the first used as nano reinforcement in 1985 by Toyota [2]. Natural form of clay is called bentonite which is produced by the alteration of volcanic ash. Bentonite contains mainly montmorillonite, MMT but also illite, kaolinite, quartz and zeolite.

Regular stacks of alumina silicate layers with high aspect ratio and large surface area is the characteristic structure of clays. Specifically, MMT has 2:1 layered structure which is consisting of tetrahedral sheets in which a silicon atom is surrounded by four oxygen atoms and octahedral sheets in which a metal such as aluminum or magnesium is surrounded by eight oxygen atoms. Figure 1.2 shows the layered structure of MMT in which thickness is about 0.97-1 nm [3].

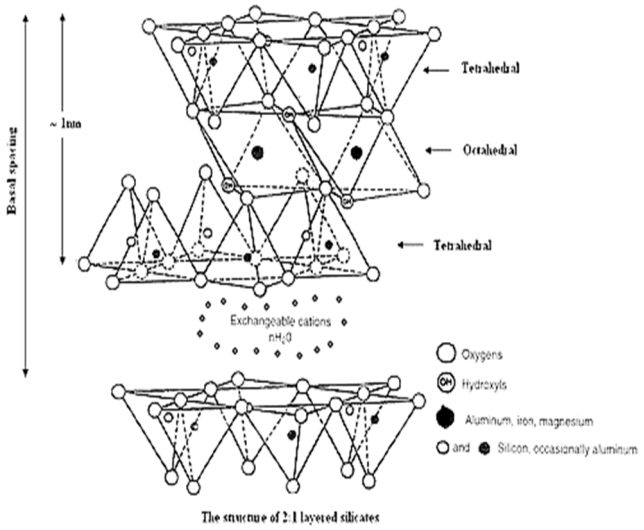


**Figure 1.2.** Crystal structure of montmorillonite [3]

Pristine form of the layered silicate is hydrophilic which means that the effective interaction between the most of the engineering polymers and the clay is impossible. Thus, the improvement in polymer properties cannot be achieved as required. By modifying the clay structure chemically, desired interactions can be reached. Several studies on modification techniques of montmorillonite appeared in the literature. The main idea in all these techniques was to produce a reactive side which generates a convenient interphase in the clay structure. Some of the researchers used montmorillonites in which the metals (Na, Mg, Al) in the galleries were exchanged by alkyl ammonium salts with long alkyl chain side groups. Kumar S. et al. studied the effects of organically modified MMTs such as Cloisite 30B, C25B and C10A on the thermal properties of PMMA [4]. The organic modifier in Cloisite 30B is methyl tallow bis-2-hydroxyethyl ammonium and the modification agent of Cloisite 25B is dimethyl hydrogenated tallow 2-ethylhexyl ammonium, whereas benzyl (hydrogenated tallow alkyl) dimethyl salt with bentonite is the organic modifier of Cloisite 10A.

In order to improve the adhesion between the nanoclay and the polymer matrix compatibilizing agents are used. Kumar M. et al. used different compatibilizing

agents such as polypropylene grafted maleic anhydride (PP-g-MA), polyethylene grafted maleic anhydride (PE-g-MA) and polystyrene grafted maleic anhydride (PS-g-MA) in PMMA/MMT nanocomposites [5]. Compatibilizer acts as a bridge between the polymer matrix and the clay layers. The organic side of the compatibilizing agents can interact with the polymer matrix and another side can exhibit strong interaction with the clay layers. The interaction between MMT and polymer affects the structure and hence the properties of the resulted product. For example, by increasing the interphase attraction of these two components, the enhancement in the mechanical and the thermal properties occurs because of the effective load transfer between them.

When the clay is mixed with the polymer matrix, different structures can be resulted depending on the interphase attraction. If the interaction between the matrix and the reinforcement is limited, then the layers of the clay cannot be distributed through the matrix, hence the improvement in the properties is restricted. This type of composites is called phase separated micro composites (Figure 1.3a). Apart from this classical composite structure, two types of nanocomposites, intercalated and exfoliated structures are revealed when clay layers start to interact with the polymer chains. In the intercalated nanocomposite, small amount of polymer chains enters into the galleries and causes increase in the distance between the layers (Figure1.3b), but the order of layers cannot be destroyed restricting the improvement in the properties of the polymer. The greatest enhancement can be reached when the clay layers are dispersed individually and randomly in the matrix (Figure 1.3c). In this case, the improvement can be very high as a consequence of the maximum level of interaction between the chains and the layers. Also, mixed exfoliated and intercalated structures can be obtained during the preparation of nanocomposites (Figure 1.3d).

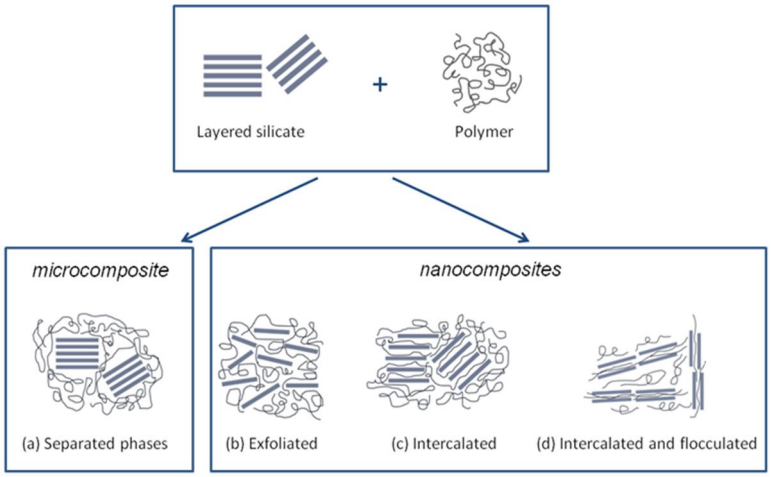


**Figure 1.3.** Possible structures resulted from mixing of clay and polymer [6]

To analyze nanocomposite structures, generally X-ray diffractometer (XRD) and transmission electron microscopy (TEM) techniques are used. If the structure is exfoliated, XRD peaks are disappeared indicating that the interlayer space is very large to be calculated at this angle range. However, TEM images should also be used to support this result. For intercalated nanocomposites, XRD peaks shifts to lower angles indicating expansion of the interlayer space between layers due to the entrance of polymer chains into the galleries.

### 1.1.2. Preparation of Polymer/Clay Nanocomposites

The structure of the nanocomposites is affected by the type of preparation techniques. Melt intercalation, solution intercalation and in situ polymerization are three main types of the preparation methods.

#### a) Melt Intercalation

This method was firstly used by Vaia et al. in 1993 for the preparation of PS/OMLS (organically modified layered silicate) nanocomposite which resulted

as intercalated structures [7]. In this technique, clay and polymer are mixed by extruder or a mixer at molten state temperature. As solvent is not needed, this technique is environmentally friendly, applicable to industry and economical. But, during the process, mixer types, modification agents of the clay and processing conditions should be chosen properly in order to obtain good quality nanocomposite.

**b) Solution Intercalation**

Aranda and Ruiz-Hitzky were first used this technique to prepare polyethylene oxide/MMT nanocomposites with different solvents [8]. This technique is conducted by dissolving the polymer in a suitable solvent and then adding clay into the solution. Sometimes, to obtain more exfoliated the clay layers, pre-mixing of clay can be ultra-sonicated in a sonication bath. Nanocomposite material can be obtained by the evaporation of the solvent or precipitation of the nanocomposites. Solution mixing is not used in industry as the technique is time consuming, harmful to environment and also expensive. However, it can produce more exfoliated structure than the melt intercalation method can. The work of Fu J., showed that the solvent co-precipitation method was a better technique than the melt mixing method producing a more exfoliated structure in PMMA/Clay nanocomposite with better mechanical properties [9].

**c) In-situ Polymerization**

This is the most effective technique for obtaining exfoliated structure in polymer nanocomposite. The first step of preparation is the swelling of nanoclay in the monomer solution. Then, monomer starts to diffuse into interlayer spaces of clay layers where the polymerization reactions will take place by the help of heat or radiation. At the end, disordered clay layers are obtained by the growth of polymer chains. This method is also not used in industry due to the same reasons encountered in solution intercalation. It is mostly performed in laboratory

researches. Usiki A. et al. performed in situ polymerization to prepare nylon6/MMT nanocomposite from ε-caprolactam monomer and MMT and found that even non-modified MMT shows intercalative structure with polymer chains [10].

### 1.2. Boron Compounds as Flame Retardants

Boron compounds like zinc borate, boric acid, boron oxide and others are used in polymeric materials as flame retardant materials. They are chosen because on the contrary to other flame retardants like halogenated compounds which produce toxic gases under burning, boron compounds are non-toxic and environmental-friendly. They can also prevent further pyrolysis of the polymers by lowering the heat flow. Table 1.1. summarizes the type of boron compounds and the common application areas in which they are widely used as flame retardants.

**Table 1.1.** Boron compounds as flame retardants [11].

| **Compound** | **Application** |
|---|---|
| Borax Pentahydrate | Wood, cellulose, cotton, coating |
| Boric Acid | Wood, cellulose, cotton, polymer, coating |
| Boric Oxide | Engineering polymers |
| Calcium Borate | Rubber modified roofing membrane |
| Zinc Borate | Polymer, elastomers, coating, sealants |
| Boron phosphate | PPE/Polyamide, PPE/HIPS, PO |

Several studies appeared in the literature on application of boron compounds as flame retardants in polymers [12-15]. Zinc borate was widely studied because its dehydration temperature is relatively high, about 290 °C, which affects both condensed and gas phase mechanism of flame retardancy. During combustion,

zinc borate can release chemically bonded water molecules as a result of dehydration which causes the flame dilution. Also, at high temperatures, glassy borate layer can be formed which protects the polymer from further oxidative degradation. Furthermore, this material can produce carbon and boron carbide based char under the glass layer [12-15].

### 1.2.1. Boronic Acids

Boronic acids produce water molecules like zinc borate during thermolysis and form boraxine or boronic acid anhydride. When more than one boronic acid functional group exists, boraxine glass structure can be generated by the elimination of water at high temperatures. This glassy network structure leads to formation of char layer on the polymer surface in which oxidation of carbon is restricted by limiting the accessible oxygen. One of the examples of boronic acids is 1,4-benzenediboronic acid whose chemical and glassy network structure are seen in Scheme 1.1.

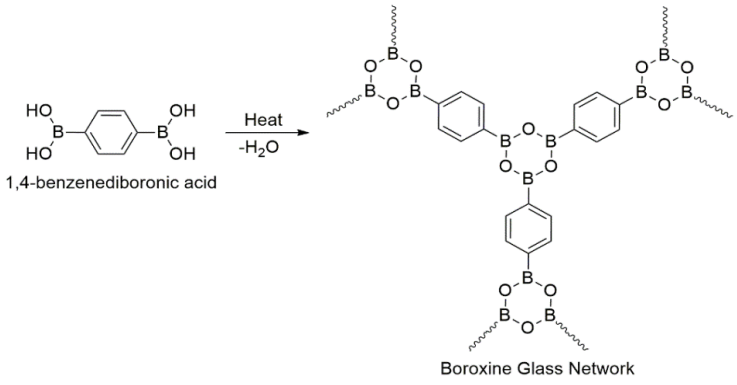


**Scheme 1.1.** Boraxine glass network structure [15]

Trans-esterification reaction is also possible between hydroxyl groups of boronic acid and alkoxy or alkoxy groups producing boronic ester structure [16]. The effect of boronic acid on thermal and flame retardant properties can be resulted

chemically by crosslink formation as well as physically by char layer construction.

## 1.3. Poly(methyl methacrylate), PMMA

PMMA is a thermoplastic polymer and has a great value in the engineering applications. It is a transparent material which can be found in the market as granules and sheet forms. It was developed in 1928 by William Chalmers, Otto Röhm and Walter Bauer and after five years it was commercialized by the German Company Rohm and Haas [17]. PMMA is also known as acrylic or acrylic glass with the trade names Plexiglas, Acrylite, Lucite and Perspex [18-20].

### 1.3.1. Synthesis of PMMA

PMMA can be synthesized by free radical polymerization reaction of methyl methacrylate (MMA) monomer by an initiator. The radical polymerization of MMA can be performed homogeneously, by bulk or solution polymerization, or heterogeneously, by suspension or emulsion polymerization. Scheme 1.2 shows the free radical polymerization pathway of PMMA. Free radical polymerization is more practical and absolute dryness is not needed. However, the oxygen in the environment must be removed because it destroys the radicals and terminates the reaction before the expected time. Radicals can be produced by radiation, heat or chemical agents for example benzophenone, azobisisobtyronitrile (AIBN), benzoyl peroxide etc. Moreover, anionic polymerization can be used to synthesis PMMA but this technique needs extra care in terms of dryness and temperature.

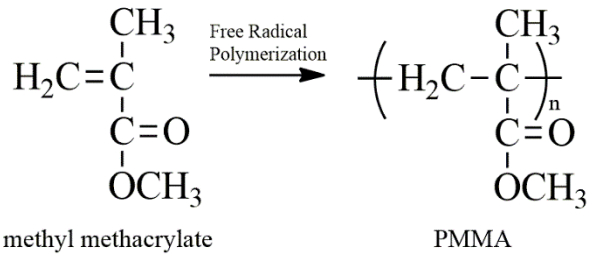


**Scheme 1.2.** Free radical polymerization reaction of PMMA

### 1.3.2. Properties of PMMA

PMMA has unique properties which affect the processing and applications. The chemical structure of PMMA as in Scheme 1.2 has large pendant groups which can lead to restriction in crystallization of PMMA chains. These large groups prevent the close attraction between the chains which leads to amorphous structures in the morphology. Moreover, large pendant groups restrict slipping over of chains from each other. As a consequence, PMMA is a rigid and brittle material with high glass transition temperature (~105 °C) and little mold shrinkage [22]. Addition of methacrylic acid increases the glass transition temperature for high temperature applications such as lightening. Brittle nature of PMMA can be reduced by copolymerization with polybutadiene or by blending with a high impact polystyrene. PMMA/PVC alloys have higher impact and stiffness than pure form of PMMA [23].

The mechanical properties of PMMA are also remarkable for many applications. It is one of the hardest thermoplastic with a high strength, high Young's modulus and low elongation at break. It has also higher scratch resistance than similar polymers like polycarbonate (PC) but glass is still better material for this property. Also PMMA is economical alternative of PC when the high strength is not needed. Some mechanical properties of PMMA are listed in Table 1.2.

**Table 1.2.** Mechanical properties of PMMA [24]

| | |
|---|---|
| Tensile Strength | 47-79 MPa |
| Elongation at Break | 1-30 % |
| Tensile Modulus | 2.2-3.8 GPa |
| Hardness, Rockwell M | 63-97 |

High transparency of PMMA makes it an ideal material for use instead of glass when the impact or weight is of serious concern. In the visible range from 380 nm to 780 nm, PMMA can transmit 92% of the light and filter trace amount of the UV light at wavelengths below about 300 nm. This small amount of absorption which eliminates the breaking down the molecular bonds with in the chain gives a unique property to PMMA such as long term weather resistance. Therefore, PMMA is well suited with automotive rare lights, aircraft cockpits and windshield. Also, because of transparency and good compatibility of PMMA with the human tissue, it can be used in replacement of intraocular lenses and contact lenses. Additionally, it can be an alternative material for denture applications because of the same reasons [25]. By the help of the colorless nature, PMMA can be easily colored with the dyes and pigments for decorative applications and protection from UV light.

Water absorption capacity of PMMA is low thus it is a suitable candidate for electrical engineering applications. Also, dielectric properties are very good but not as in the PS and LDPE ones. This feature depends on the temperature and relative humidity of the ambient. Some electrical properties are illustrated in Table 1.3.

**Table 1.3.** Electrical properties of PMMA [24]

| | |
|---|---|
| Electrical Resistivity | $10^{14}$ - $10^{15}$ Ω.cm |
| Dielectric Constant | 2.8 - 4 |

Aqueous solutions such as dilute inorganic acids, alkalis, detergents, cleaners etc. cannot affect PMMA, however it cannot be used in the presence of chlorinated or aromatic hydrocarbons, esters or ketones. Acetone, chloroform and di-chloroethane dissolve the polymer completely.

The most problematic feature of the PMMA is the thermal characteristics. It is combustible and burns easily generating heat, smoke and toxic gases. At elevated temperatures, PMMA applications are limited because of the poor thermal stability. This is the basis of the most of the research on the composite and nanocomposite forms of PMMA.

### 1.3.3. Thermal Degradation Mechanisms of PMMA

Thermal degradation of PMMA has been analyzed in several studies [26-29]. Manring et all. found out that different steps involved during the thermal degradation of PMMA [26]. Firstly, thermal degradation of PMMA starts with the breaking off weak head to head bonds (H–H) which promotes to the facile homolytic chain scissions around 270–300°C (Scheme 1.3). However, the presence of the large steric hindrance and the inductive effects of the ester groups reduce the rate of the main chain scission mechanism and restrict the effect of these H-H bonds.

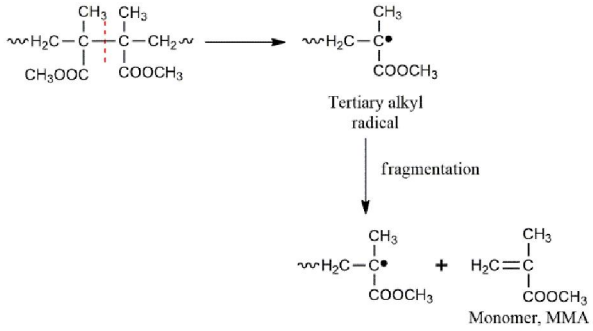


**Scheme 1.3.** Homolytic chain scission of PMMA yielding the monomer.

Secondly, due to the unsaturated end groups of PMMA, there are two weight loss processes at around 180 and 270°C. Radical transfer to the vinyl chain end initiates the degradation of PMMA through chain transfer processes. Elimination of unsaturated chain end produces radical chains which continue further decomposition yielding the monomer (Scheme 1.4). Therefore, any free radicals due to presence of impurities, H-H bonds, scissions β to the vinyl group at unsaturated ends and/or random scission can produce the monomer as the degradation product.

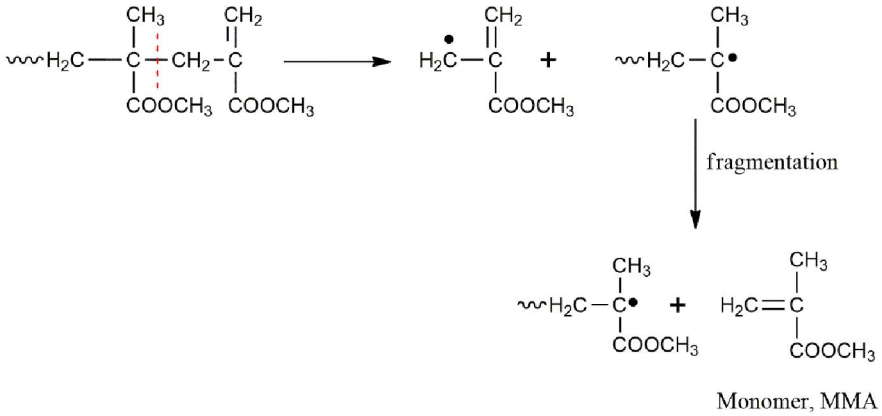


**Scheme 1.4**. Elimination of the unsaturated end groups of PMMA yielding the monomer.

Lastly, in addition to the main chain scission, random and homolytic scission of methoxycarbonyl side groups followed by β scission would be seen during the degradation of PMMA at around 350-400°C (Scheme 1.5). Methoxycarbonyl side group can react with the H radicals producing $CH_3OH$ and $CH_4$ molecules. Compared to the other two mechanisms, the random side group scission is the least important one in the thermal degradation processes of PMMA [26].

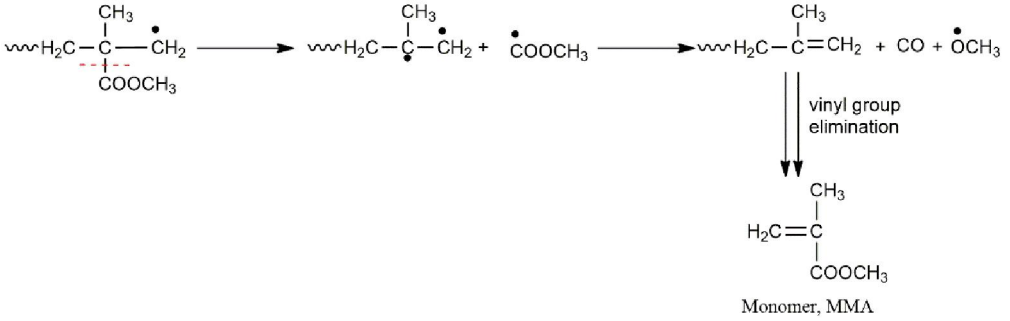


**Scheme 1.5.** Random side group scissions in PMMA.

This mechanism is also predicted for the char formation during the combustion of PMMA. Char formation can be resulted from the side chain elimination and following structure (Scheme 1.6.) is assumed to be the char structure of PMMA and formed products [26].

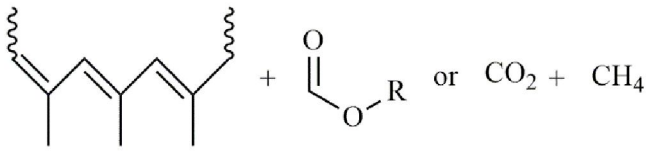


**Scheme 1.6.** Proposed structure of PMMA char and resulted products

In the presence of oxygen, thermal oxidative decomposition of PMMA can takes place which causes formation of hydro peroxides from the interaction of oxygen

and macro radicals [29]. This is unstable and leads to generation of more free radicals. Thermal oxidative degradation mechanism was studied by Song et al [28]. The main product is again monomer but additionally, 2-methyl-oxirane carbonic acid methyl ester, methyl pyruvate and dimethyl itaconate can be resulted. MMA monomer can also subject to further decomposition which gives smaller gaseous products like $CO_2$, CO. [29].

Thermal stability of PMMA can be increased by copolymerization, crosslinking and using some additives in macro, micro and nano size.

### 1.3.4. Poly(methyl methacrylate) Nanocomposites

Nano size reinforcements have significant effects on the properties of the polymers if they are finely distributed through the matrix. Because of the reinforcement in nano size, the interaction between the polymer and the reinforcement is at molecular level. Therefore, strong molecular interactions can be obtained through each polymer chains and nano additives which promotes the enhancement of specific properties of the polymers. This is also called “nano effect”. Material in nano size is much stiffer and stronger than micro size because of the decrease in the possibility of defects in the materials and the elimination of weak secondary bonds.

To improve the mechanical, thermal, electrical, flame and barrier properties of PMMA, some nano additives are incorporated into PMMA matrix. The most commonly used additives in PMMA matrix are nanoclays, carbon nanotubes, nanosilica, zirconia nanoparticles, and nano-boron nitride(n-BN). Matoung’s research group found that addition of zirconia particles affects the thermal stability of PMMA by increasing the degradation temperature [30]. Elimat et al. examined the effects of calcium carbonate ($CaCO_3$) on optical properties of PMMA and observed increase in the thermal conductivity of PMMA matrix by addition of 2% nanofiller [31]. PMMA and multi-walled carbon nanotube

(MWCN) composite were prepared and characterized for gas sensing applications and the results revealed improvement in resistance to some chemicals for the nanocomposite structure with respect to pure form of PMMA [32]. In addition to all of these nanofillers, the mostly used one in PMMA matrix is nanoclay.

### 1.3.5. Effects of Montmorillonite on Properties of PMMA

#### a) Mechanical Effects

Addition of montmorillonite (MMT) into PMMA matrix can improve the mechanical properties of the polymer if interfacial bond formation between matrix and reinforcement is sufficient. The applied load on the weaker matrix can be transferred to the stronger and stiffer reinforcements. Also, adding MMT can lead to decrease in the chain mobility of PMMA so chains cannot move freely under mechanical loading. Kumar M. et al. found that the tensile modulus was improved about 16-20% by the help of effective stress transfer from matrix to reinforcement for PMMA/clay nanocomposite modified with a compatibilizer [5]. However, tensile strength of the nanocomposites in this study was lower than pure PMMA. Clay loading caused further brittleness in the matrix due to presence of some tactoid formation in the morphology. Another important mechanical property is the hardness. MMT can restrict the indentation and lead to improvement in hardness, due to its high strength. It was found that hardness is enhanced about 34% by clay loading [5]. The amount of clay is found to be very critical parameter in this study, as high level of loadings can produce some agglomeration in the structure which will cause weaker mechanical properties. This is still most problematic issue in nanocomposite science and it is tried to be solved by examining different preparation methods, modification techniques and other ways.

**b) Thermal Effects**

Another important effect of MMT is the improvement in thermal characteristics of PMMA. Due to inorganic nature of MMT, char formation can be seen during degradation process, as at the degradation temperatures of PMMA, clay mineral can preserve its thermal stability in the form of char residue. Char residue acts as a barrier which can stop the evaporation of small volatile molecules during the degradation of PMMA matrix. Hence, the thermal degradation temperatures are shifted to higher values as shown in the study of Boudjemaa research group [33]. They used organically modified MMT with alkyl ammonium salts at different amounts of loading and found that as the amount of clay added was increased, the enhancement about 7% in decomposition temperature can be achieved. In addition, the glass transition temperature shifted to higher values because of the effect of MMT on the chain mobility of PMMA [33]. Di Pasquale and coworkers [34] observed improvement in thermal properties of PMMA by adding MMT organically modified with imidazolium salt. The improvement in this case was much greater, as 17%, due to the better thermal stability of imidazolium salts than the alkyl ammonium salts [34]. Clay loading also affects the thermal conductivity of PMMA as shown in the study of Pandey P. and coworkers. PMMA/clay nanocomposite materials displayed an improvement in the thermal conductivity and this behavior was correlated with the existence of clay stacks and agglomerates. In the case of effective dispersion of MMT, heat transport was restricted because of the limited local vibration of atoms and molecules in the amorphous matrix [35].

**c) Barrier Effects**

Chang K. and coworkers studied the corrosion protection behavior of MMT on PMMA matrix by electrochemical measurements. They found that nanocomposite materials exhibited lower water vapor and oxygen permeability than pure PMMA. It was concluded that clay exhibits enhanced molecular

barrier property which was a consequence of the tortuous path theory [36]. This means that clay layers construct long tortuous diffusion pathways which restrict the motion of the molecules in the material. In conventional composites, this theory is not valid because of the structure of macro and micro reinforcements. Figure 1.4 illustrates the path differences for permeability between composite and nanocomposites.

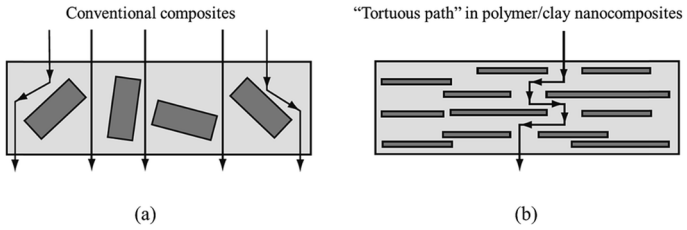


**Figure 1.4.** Torturous diffusion path" in polymer/clay nanocomposite [37]

### d) Flame Retardancy

One of the most studied property of PMMA/clay nanocomposites is the flammability characteristics. Existence of nanoclay can affect mechanism and also retard the burning process because of the influence in the condensed and gas phases. Gas phase action includes flame inhibition, fuel dilution and flame temperature lowering. For example, during burning, MMT produces noncombustible gases in large amounts diluting the combustible gases exhausted from PMMA. Also, it decomposes endothermically absorbing significant amount of heat. In the condensed phase, because of char formation, diffusion of the gas is hindered. The following figure (Figure 1.5) shows the char surface formation by the motion of silicate layers.

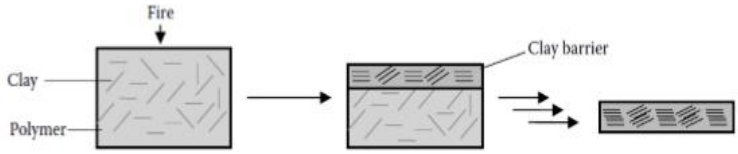


**Figure 1.5.** The schematic view of the migration of the layered silicates during burning [11]

Different kinds of techniques were applied for analysis of the flame retardancy properties of PMMA/MMT nanocomposites in the literature [35,38-41]. Pandey P. et al. showed that clay addition to PMMA caused faster burning rate with shorter time of burning [35]. However, nanocomposites burned without dripping which triggered the fire separation therefore nanocomposite materials were safer in the case of fire. Another study showed that modification of MMT with boron molecules caused increase in time of burning [39]. Same observation was observed by Huang G. and coworkers for PMMA/MMT nanocomposites in which MMT was modified with the phosphorus–nitrogen containing ammonium salt in order to improve flame characteristics [40]. These findings indicated that traditional clay like Cloisite 30B alone cannot improve flammability properties of PMMA. To overcome this problem, another method is available in which nanoclay and traditional flame retardants can be used together for "synergistic effect". In Kim S. study, triphenyl phosphate was employed as flame retardant in PMMA/clay system and it has been found that it constructed a protective layer on the surface of the polymer which yielded improvement in both thermal and flame properties of nanocomposite [41].

### 1.3.6. Effects of Boron Compounds on Properties of PMMA

Boron compounds either in the form of micro or nano size additive have important effects on the properties of PMMA as in several studies [42-45].

Kiran et al. studied the effect of BN nanosheets on the mechanical properties of PMMA and found that improvement in the mechanical properties of PMMA was obtained when the few number of BN nanolayers were added [42]. In the study of Koysuren O. and coworkers, an improvement in the thermal stability of PMMA blended with the boron containing polymer, polyvinyl borate (PVB) was detected. This was resulted from the formation of thermally more stable B-O-C bonds constructed during the blending of PVB and PMMA [43]. Boron oxide particles were used in the research of Doğan M. et al. They found that PMMA/Boron oxide nanocomposites had better thermal characteristics than pure PMMA due to the changes in the thermal degradation mechanism [44]. Another research was conducted to obtain improved optical properties of PMMA with the addition of lanthanum hexaboride ($LaB_6$) in different particle sizes. It was found that $LaB_6$ particles in the size of 70 nm showed best absorption of NIR and VIS light which could not be achieved by the composites beyond the nano scale [45].

### 1.4. Aim of the Study

In this research, our main aim is to prepare and characterize composites and nanocomposites involving organically modified montmorillonite, special one Cloisite 30B (C30B), of poly(methyl methacrylate), PMMA, containing variable amounts of 1,4-benzenediboronic acid (BDBA). Two different preparation methods, melt mixing and solution casting were employed to produce PMMA/BDBA composites and PMMA/C30B/BDBA nanocomposites involving different amounts of BDBA. The purpose of the adding OMMT to the PMMA/BDBA matrix was to create synergism between OMMT and BDBA at the molecular level which may lead to a further increase in the characteristics of PMMA. X-Ray Diffractometry (XRD), Scanning Electron Microscopy (SEM) and Transmission Electron Microscopy (TEM) analyses were performed to investigate the morphology of the composites. For thermal characterization,

Thermogravimetric (TGA) and Direct Pyrolysis Mass Spectrometry (DP-MS) analyses were operated. Moreover, mechanical and flame testing were performed by Universal Testing Machine under tensile loading, Low Oxygen Index (LOI) and UL94-V respectively.

# CHAPTER 2

# EXPERIMENTAL

## 2.1. Materials

PMMA with the trade name SUMIPEX® Clear 011 (specific gravity=1.19 g/cc) was purchased from Sumitomo Chemical Co., Ltd. Its tensile strength and elongation at break values were reported as 68.9 MPa and 7.0% respectively. Methyl tallow bis-2-hydroxyethyl ammonium modified montmorillonite Cloisite 30B (C30B) was used as nano-reinforcement material and purchased from Southern Clay Products Inc. Its cation exchange capacity is 90 meq/100g clay and interlayer space between clay layers ($d_{001}$) is 1.85 nm. Chemical structure of its organic modifier can be seen in Figure 2.1a. Benzene-1,4-diboronic acid, BDBA with the purity of 95.0% was purchased from Sigma-Aldrich Co. The chemical structure of BDBA are shown in Figure 2.1b. Solvents $CHCl_3$ (99%) and DMF (99%) were obtained from Sigma Aldrich. All materials were used without further purification.

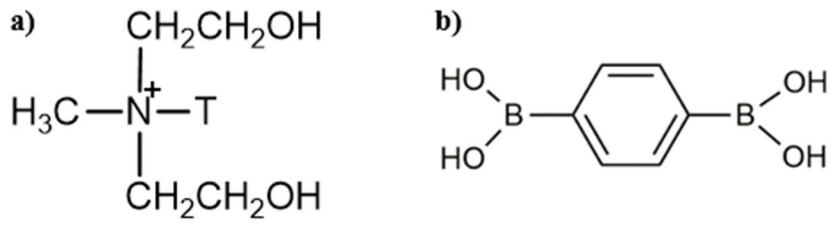


**Figure 2.1.** Chemical structures of a) organic modifier of Cloisite 30B and b) benzene-1,4-diboronic acid, BDBA.

## 2.2. Preparation of PMMA Micro and Nanocomposites

Melt mixing and solution mixing techniques were performed in order to prepare PMMA/BDBA and PMMA/C30B/BDBA nanocomposites. The effect of preparation methods on the properties of the materials was analyzed. Before mixing, all the materials were dried at 60 °C in vacuum oven. Table 2.1 shows the composition of composites prepared by both techniques.

**Table 2.1.** Composition of PMMA composites prepared

| Compounds | Weight % of Additives | |
|---|---|---|
| | BDBA | C30B |
| PMMA/BDBA | 1, 3, 5, 7, 15* | |
| PMMA/C30B | | 3 |
| PMMA/C30B/BDBA | 1, 3, 5, 7, 15* | 3 |

* only prepared by solution mixing

### 2.2.1. Melt Mixing

After drying, PMMA and the additives were mixed in a DSM Xplore twin screw micro compounder. Before extrusion, polymer and additives were pre-mixed in order to prevent non-uniform distribution of additives. Then, they were continuously poured into feeding zone of extruder and mixed at 100 rpm screw speed for 3 min at 200 °C process temperature. At the end, 15 g of ten different blends were prepared.

#### a) Injection Molding

After extrusion, injection molding was applied in order to obtain tensile test specimens with the length (L), width (W), and thickness (T) as 50 mm, 7.6 mm, and 2 mm, respectively. Before the injection, all the compounds were dried at 65

°C for 2 hours. During the process, 210 °C barrel temperature, 40 °C mold temperature and 10 bar pressure were performed by Microinjector, Daca instrument to obtain identical dog bone shaped materials as shown in Figure 2.2.

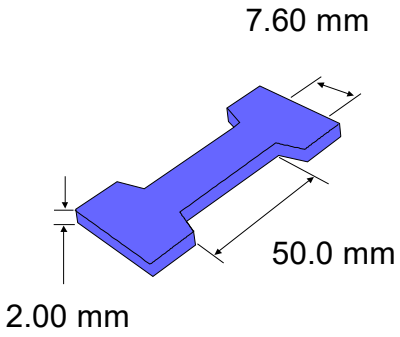


**Figure 2.2.** Schematic representation of tensile test specimen

**b) Compression Molding**

In order to obtain LOI and UL94-V values, flammability test specimens were prepared by compression molding. For LOI tests, dimensions of the specimens were 130 ×6.5 × 3.25 $mm^3$ and for UL-94V tests, dimensions of the specimens were 130 × 13 × 3.25 $mm^3$. Firstly, the materials were pre-heated in heated open mold cavity, and then samples were heated in a closed cavity under high pressure at 200 °C. After molding, samples were removed from the cavity and cooled at room temperature.

### 2.2.2. Solution Casting

In this technique, 2 g of compounds were prepared by dissolving the desired amount of filler and PMMA in 25 mL DMF solvent. For incorporation of OMMT into PMMA matrix, firstly, 3 wt% clay in 25 mL DMF was pre-mixed about 30 min in an ultrasonic bath, Elma Ultrasonic Processor LC30, to obtain

clay layers more separately. After ultrasonic mixing, boron compound and PMMA were added into the solution and mixed by magnetic stirrer about 24 hrs. Then, the solutions were casted into petri glasses and left to dry in air for 24 hrs and then further dried at 150 °C for 30 min in vacuum oven. At the end, products were in the form of film structure.

### 2.3. Characterization Methods

To analyze the morphological, thermal, mechanical and flame retardancy properties of PMMA composites different characterization methods were applied.

#### 2.3.1. Morphological Analyses

XRD and TEM analyses were utilized to gain the information on micro or nano structure of the polymer nanocomposites. SEM device was used to visualize the surface structure of PMMA/BDBA micro composites.

##### 2.3.1.1. X-Ray Diffractometer (XRD)

In this study, to analyze 2θ XRD patterns of PMMA composites, Rigaku X-ray diffractometer (Model, Miniflex) with CuKα (30 kV, 15 mA, λ = 1.54051 Å) was used at room temperature. XRD patterns were scanned in the range 1° to 30°.

##### 2.3.1.2. Transmission Electron Microscope (TEM)

TEM analysis offers direct images of the dispersion of nanofillers within the polymer matrix and is a qualitative analysis to view morphological structures of

clays in polymer matrix. The basic principle of the TEM analysis depends on the interaction of a beam of electron with the ultra-thin layer of samples.

TEM analyses were performed by using a FEI Tecnai G2 Spirit BioTwin CTEM. For the nanocomposites obtained by melt blending, ultra-thin sections of dog bone shaped products were prepared by ultramicrotomy process. On the other hand, for the blends prepared by solution casting, very dilute solutions of nanocomposites in $CHCl_3$ were poured into carbon coated-cupper grid with 3 mm diameter and 400 mesh. Then, the grid was allowed to dry in room temperature for 24 hrs. After drying, TEM analyses were performed.

#### 2.3.1.3. Scanning Electron Microscopy (SEM)

SEM is a practical technique to study the morphology of the micro particles. The information about the dispersion and the surface characteristics of BDBA particles were analyzed. Microstructure analyses of the composites were performed by QUANTA 400F Field Emission scanning electron microscope. Samples were coated with 5 nm Au/Pd (PECS-682) prior to the SEM imaging.

### 2.3.2. Thermal Analyses

Thermal analysis is a technique in which a physical property of a substance measured as a function of temperature, while the substance is subjected to controlled heating.

#### 2.3.2.1. Thermal Gravimetric Analysis (TGA)

In TGA analysis, a certain amount of sample is heated as a function of time and the change in weight is measured. TGA is commonly used to study polymer degradation reactions. TGA were performed by Perkin Elmer Instrument

STA6000 under inert medium which was obtained by flowing nitrogen gas at a rate of 20 mL/min. 5 mg of samples were heated from room temperature to 650 °C with a rate of 10 °C/min.

#### 2.3.2.2. Direct Pyrolysis Mass Spectrometry (DP-MS)

In DP-MS technique, the material is pyrolyzed in an inert medium and the high vacuum system immediately removes the decomposition products from the heating zone. Therefore, secondary and condensation reactions are almost totally eliminated. Total ion current (TIC) curve, the variation of total ion yields as a function of temperature is recorded. Thermal degradation productions as a function of volatilities and thermal stability can be identified. However, in general, incorporation of the mass spectra of polymers is very complicated due to the further decomposition of the fragments during ionization and generation of fragments with same mass to charge ratio but different chemical formula. Thus, the variations in evolution profiles, the change in relative yields of fragments as a function of temperature, are analyzed.

DP-MS analyses were performed by using Waters Micromass Quattro Micro GC Mass Spectrometer with a mass range of 10 to 1500 Da coupled to a direct insertion probe system. During the pyrolysis, temperature was increased to 50 °C at a rate of 5°C/min and then increased to 650°C with a rate of 10°C/min and kept at 650°C for an additional 5 minutes. 100 mg composites prepared by melt blending or solution casting were dissolved in 2 mL chloroform or DMF. From this solution, 2µL sample was put into the flared quartz sample vials and allowed to dry at room temperature until all the solvent was evaporated. Then, it was pyrolyzed while recording 70 eV EI mass spectra at a mass scan rate of 1 scan $s^{-1}$. Each sample was analyzed at least twice in order to evaluate the reproducibility of results.

### 2.3.3. Flammability Tests

Flame characteristic of PMMA and its micro and nanocomposites was measured by LOI and UL94 tests.

#### 2.3.3.1 Limiting Oxygen Index (LOI) Flame Test

To determine the limiting oxygen index, LOI, test specimens are burned in a mixture of oxygen and nitrogen containing medium. For most of the commodity polymers LOI ranges between 17% and 25%; above 27%, self-extinguishing could be observed. By using Dynisco Limiting Oxygen Index Analyzer instrument, LOI values were determined according to the standard oxygen index test ASTM D2863.

#### 2.3.3.2. UL-94V Flame Test

In the Underwriter Laboratory (UL) 94 test, a sample is ignited at the bottom and burned vertically. Finally, the material is classified according to the flame time, dripping and ignition of the underlying cotton as classified gradually from V-0 (best classification) to V-1, V-2, and NC (not classified). UL-94V tests were performed by on sample bars of specified size according to ASTM D3801.

### 2.3.4. Mechanical Test

The mechanical tests consist of the analyses of the tensile properties of unreinforced and reinforced polymers in the form of standard test specimens under defined conditions of pretreatment, temperature, humidity, and testing machine speed. Mechanic properties of the composites were investigated by Lloyd LR 30 K universal testing machine under a tensile loading according to ASTM D638

standard. The specimen was drawn with a speed of 5 cm/min and 5 kN load cell at room temperature.

# CHAPTER 3

# RESULTS AND DISCUSSION

The morphological and thermal properties of PMMA, its composites containing only boron compound (1,4-benzenediboronic acid, (BDBA)), and nanocomposites involving both BDBA and Cloisite 30B (C30B), prepared by solution casting and melt mixing techniques were investigated. Moreover, the mechanical and flame characteristics of melt mixed composites were evaluated for the melt blended composites. The effects of amount of BDBA, the presence of clay and preparation method on the properties of PMMA were discussed systematically.

## 3.1. Morphological Analysis

To study the morphology of the samples, XRD and TEM analyses of nanocomposites containing montmorillonite and SEM analysis of PMMA/BDBA composites were performed.

### 3.1.1. XRD Analysis

#### a) PMMA/BDBA Composites

XRD patterns were recorded for composites in order to evaluate dispersion of boron and clay into PMMA matrix. Figure 3.1 illustrates XRD patterns of PMMA/BDBA composites for both solution and melt mixed compounds. The broad peak around 20° was resulted from the amorphous PMMA chains

characterizing the arrangements of macromolecules. The orders of the polymer chains were more destroyed in the presence of solvent molecules therefore the shifting to the lower angles in broad peak was more prominent for solution mixed composites. Characteristic boron peaks detected in the range of 17° to 30° disappeared in the diffractograms of both solution and melt mixed composites. However, for the solution mixed composite involving 15 wt% BDBA, the broad peak above 25° may be associated with the unaffected crystal structures of boron remaining in the polymer matrix. However, the disappearance of the sharpness of BDBA peaks indicated that the crystallinities of the most of the boron particles were destroyed.

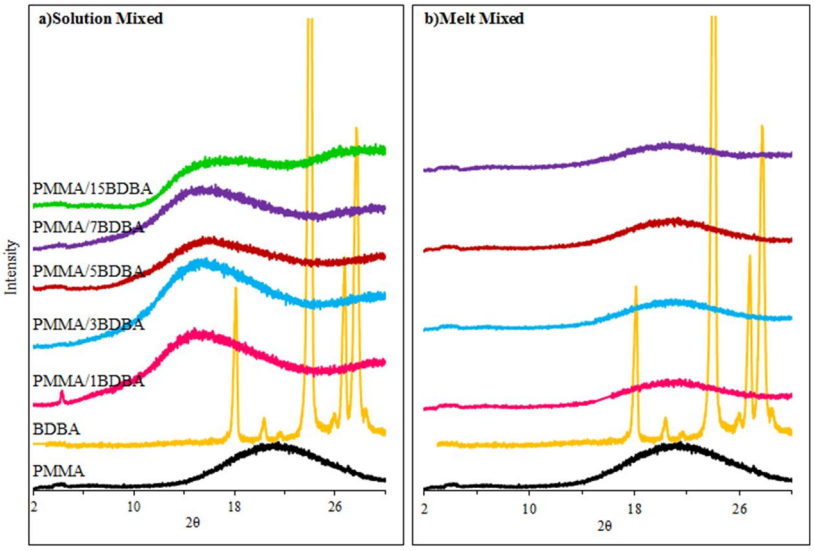


**Figure 3.1.** XRD patterns of PMMA/BDBA composites prepared by melt and solution mixing.

### b) PMMA/C30B/BDBA Nanocomposites

For PMMA/C30B/BDBA nanocomposites, the XRD patterns were recorded between 2θ=2-8° and the separation of the clay layers and the dispersion of

BDBA particles were analyzed. Figure 3.2 shows the XRD patterns of PMMA/C30B/BDBA nanocomposites produced by solution mixing and melt blending. The diffractogram of C30B has a distinct maximum around 2θ=5.06° corresponding to an interlayer distance of $d_{001}$=1.8 nm. This peak is shifted slightly to 4.35° for the solution mixed PMMA having 3 wt% C30B, indicating only a slight increase in the interlayer distance to 2.0 nm. However, for the composites involving variable amounts of BDBA, this peak is totally disappeared. However, the XRD pattern of the 15 wt% BDBA nanocomposite prepared by solution casting shows a broad peak around 2θ=6.5° which may be resulted from the stacking of the boron particles or the interaction between BDBA and organic modifier of montmorillonite which may reduce the interlayer space of the nanoclay. In the diffractograms of the melt mixed nanocomposites, peak related to the OMMT are not observed.

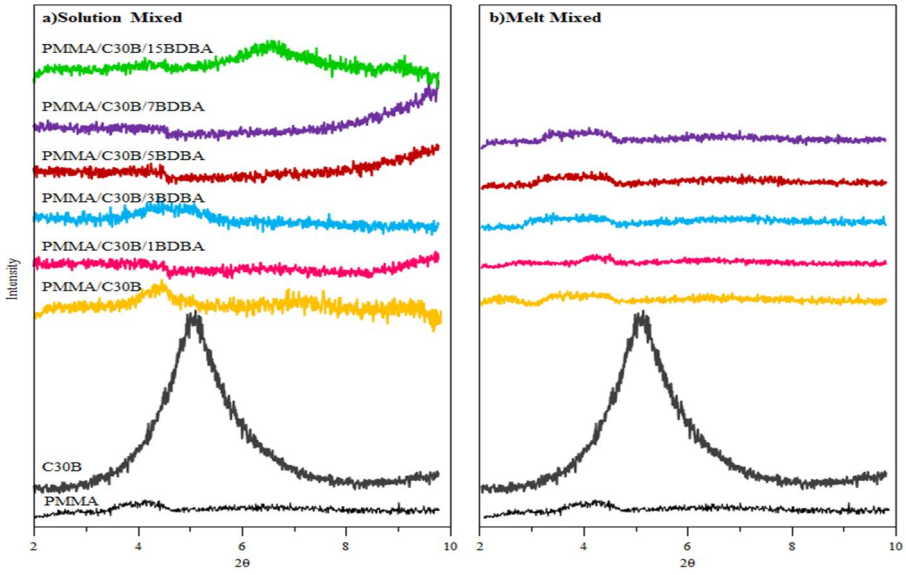


**Figure 3.2.** XRD patterns of a) solution mixed and b) melt mixed PMMA nanocomposites for the OMMT analysis.

The sharp boron peaks were disappeared in the diffractograms of all the nanocomposites prepared by both mixing techniques (Figure 3.3). Similar to what was observed in PMMA/BDBA composites, the broad PMMA peak was shifted to lower angles indicating that the regularity of the chains was destroyed especially for the solution mixed products. Therefore, according to XRD analysis, it may be concluded that the crystal structure of the nanoclay was affected in the PMMA matrix. However, the disappearance of an XRD peak does not necessarily signify that the organoclay is highly dispersed as clay dilution and several factors inducing peak broadening can lead to the disappearance of a diffraction peak.

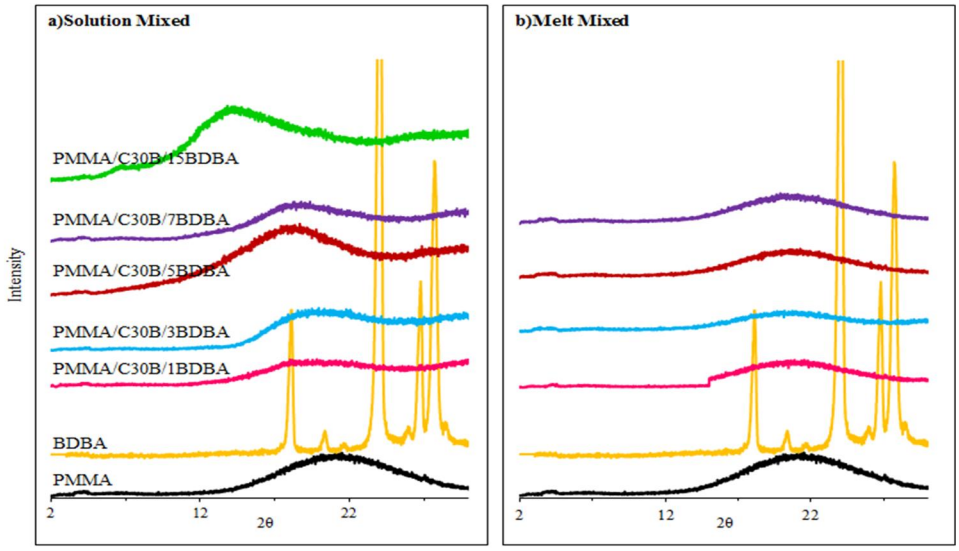


**Figure 3.3.** XRD patterns of PMMA nanocomposites for the BDBA analysis

### 3.1.2. TEM Analysis

To support XRD results, TEM analyses were performed to visualize the separation of the clay layers. TEM images of the solution and melt mixed nanocomposites are shown in Figures 3.4 and 3.5 respectively. In these images, light regions indicate PMMA matrix and the dark regions are the clay layers. The morphologies

of the clays were mostly consisting with the intercalated structures and partially exfoliated regions for the composites prepared by both techniques as can be seen in the figures. But especially for the solution casted composites more exfoliated regions can be observed. Presence of the boron particles did not cause any difference in the morphology of the nanocomposites.

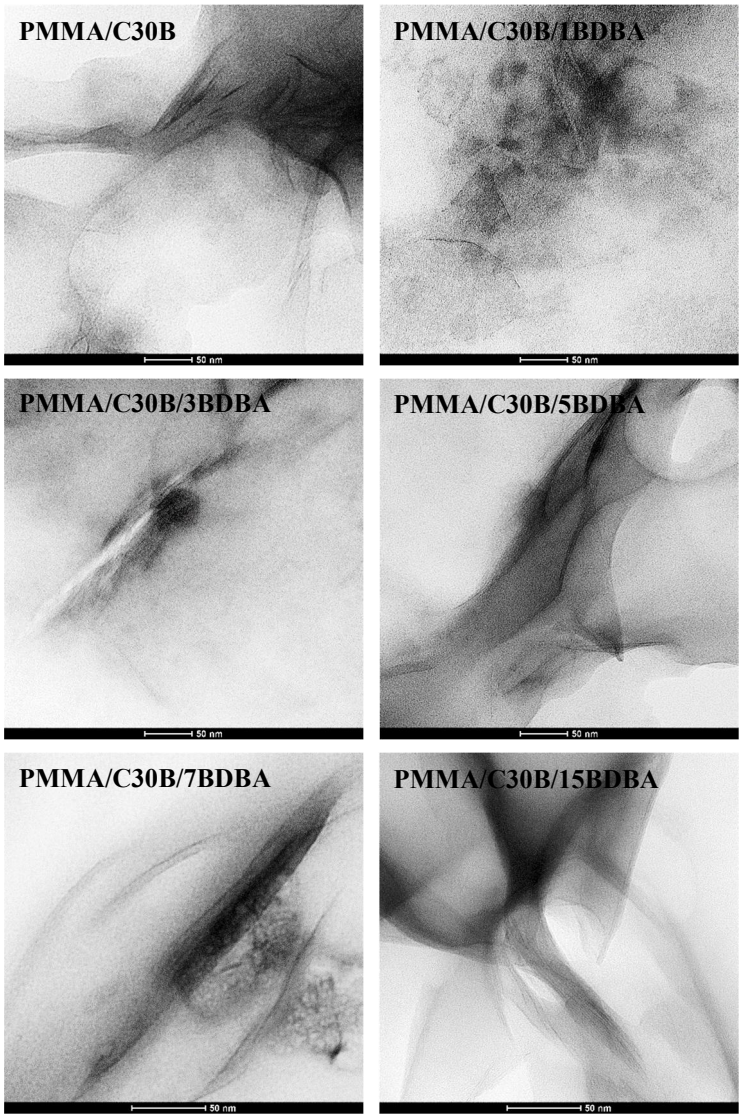


**Figure 3.4.** TEM images of solution mixed PMMA nanocomposites at 50 nm magnification

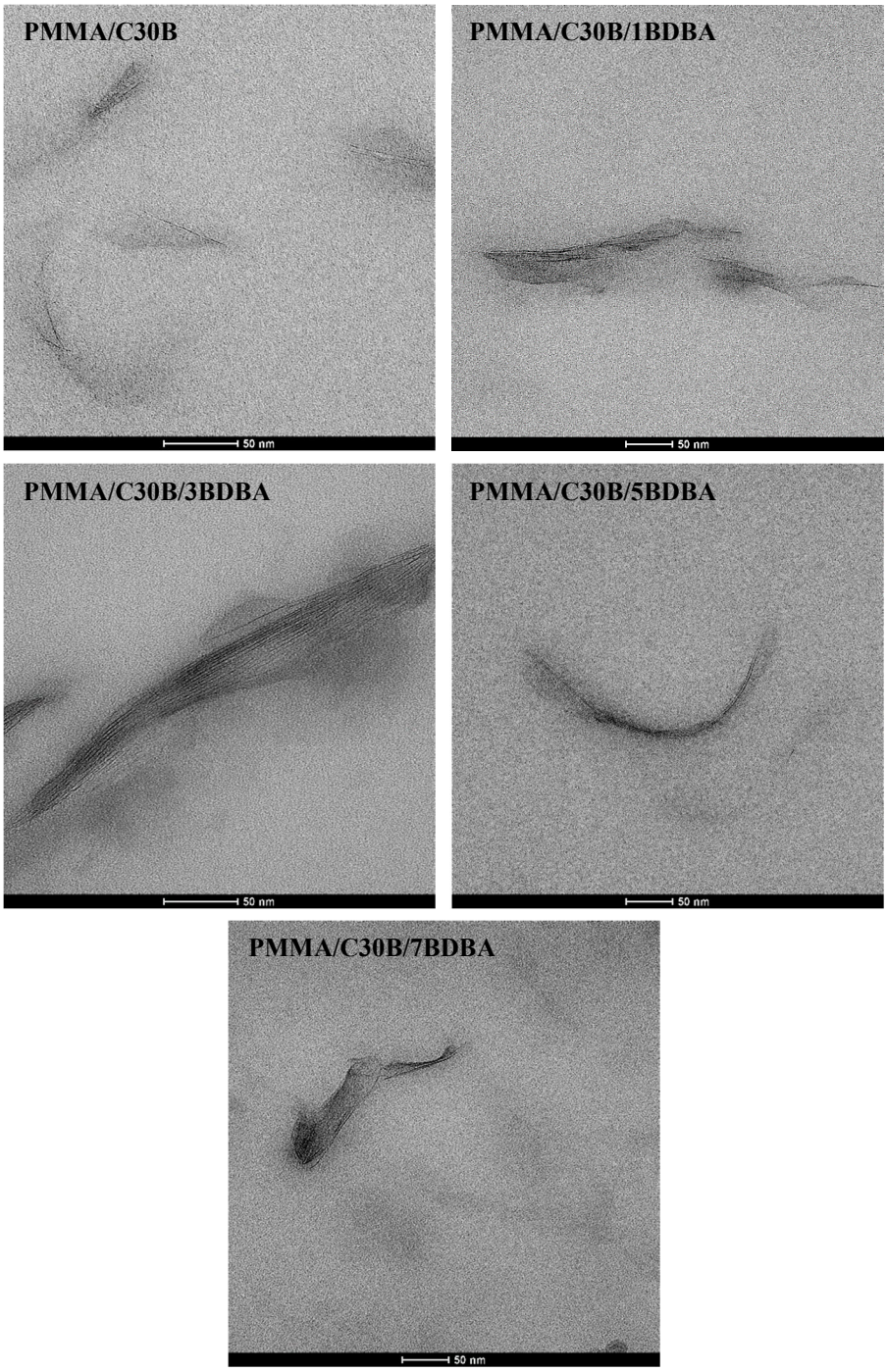


**Figure 3.5.** TEM images of melt mixed PMMA nanocomposites at 50 nm magnification.

### 3.1.3. SEM Analysis

To study the dispersion of BDBA in the solution casted composite matrices, the surfaces of the composite films were analyzed. Figure 3.6 shows the SEM images of PMMA/BDBA composites recorded at 10000 and 2000 magnifications and pure BDBA particles recorded at 10000 magnifications. In these images, dark regions indicated the PMMA matrix and white particles related with the BDBA filler. From SEM images of pure BDBA, the particle size of BDBA was found about 1.2 μm by measuring at least 10 BDBA particles. SEM images of composites at either high or low magnifications showed the agglomeration of BDBA particles in the PMMA matrix. These regions can be observed even for the composites involving low concentrations of BDBA. The separation of BDBA particles from each other may be difficult because of the high level of attraction between the boron particles. The SEM images are not sufficiently clear to conclude that the agglomeration was increased with the increase in the amount of BDBA as a big agglomerated region were not determined in PMMA/15BDBA composite at low magnification.

For the melt blends of PMMA/BDBA composites, fracture surfaces of dog bone specimens were analyzed. Figure 3.7 shows the SEM images of the melt blends at 10000 and 2000 magnifications indicating that agglomerated regions of BDBA particles in the matrix are not significant. However, it can be said that BDBA particles were dispersed more separately when the weight % of BDBA was 3 or lower. Above 3 wt%, the dispersion was restricted because of the high level of interactions between the boron particles.

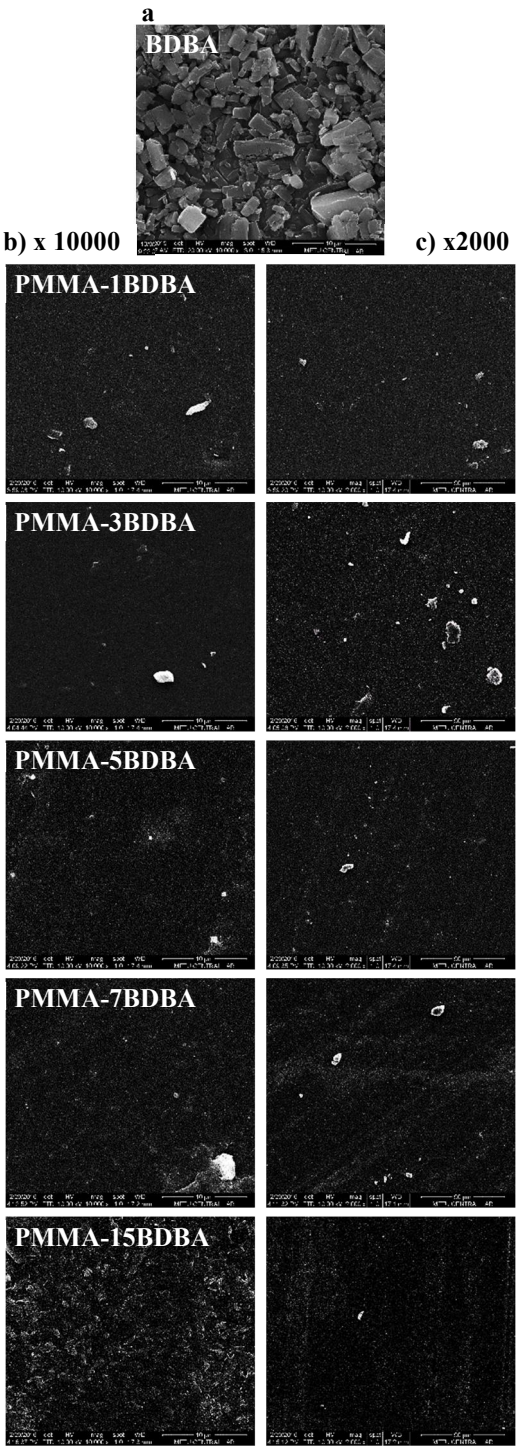


**Figure 3.6.** SEM images of a) BDBA particles at x10000 magnification and solution casted of 1,3,5,7 and 15 wt% BDBA in PMMA matrix at b) x10000 c) x2000 magnifications.

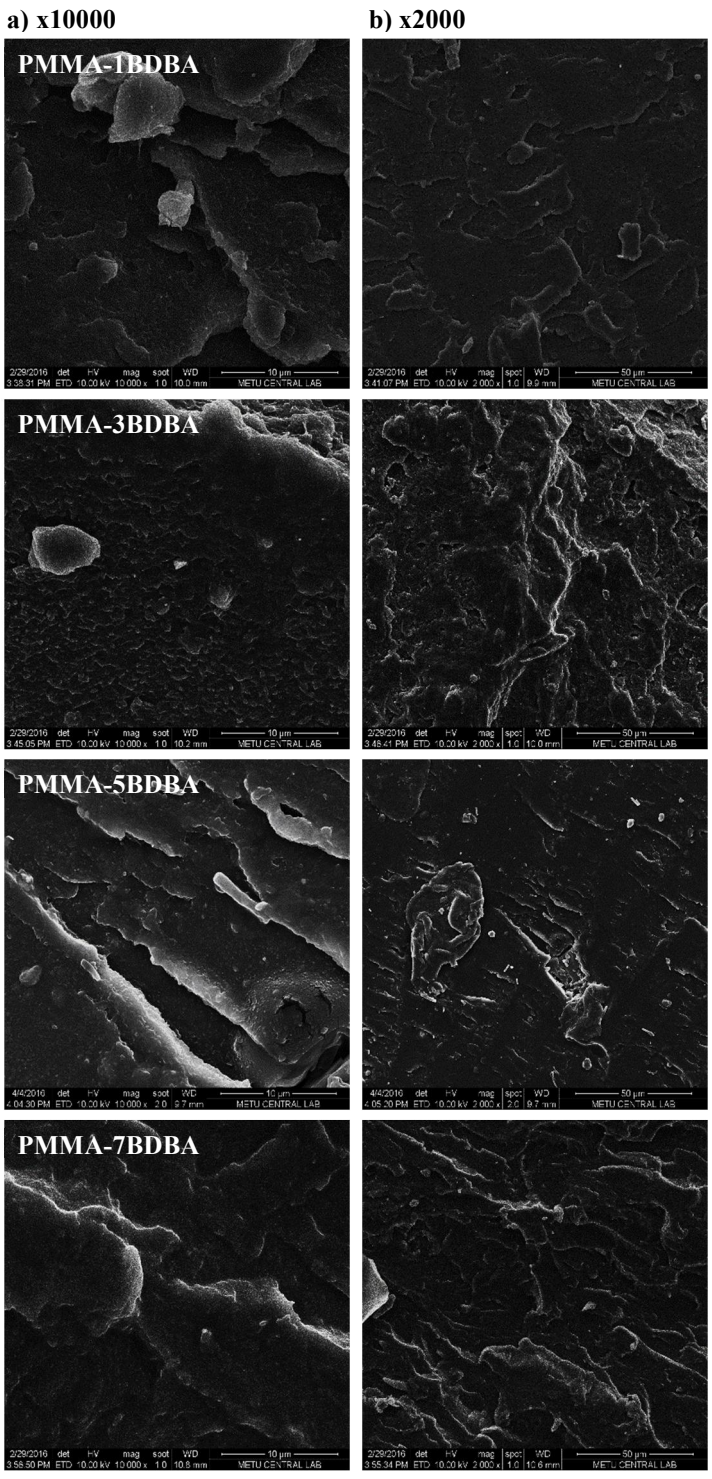


**Figure 3.7.** SEM images of melt blended of 1, 3, 5 and 7 wt% BDBA in PMMA matrix at a) x10000and b) x2000 magnifications.

### 3.2. Thermal Analyses

In order to study thermal behavior of PMMA composites, TGA and DP-MS studies were performed.

#### 3.2.1. Thermogravimetric Analyses (TGA)

In TGA, % weight loss of compounds under an applied temperature scan program was recorded and the related data are summarized in Table 3.1.

**a) PMMA/BDBA Composites**

PMMA is a kind of polymer which burns without char forming and decomposed in a single step with maximum mass loss rate of temperature at around 370°C. With the addition of BDBA particles, char formation was enhanced with respect to pure PMMA noticeably, especially for the composites involving 5 or more wt% BDBA.

TGA curves of PMMA/BDBA composites obtained by solution and melt mixing are depicted in the Figure 8 and first derivatives of %weight loss are sketched in the Figure 3.9. The temperatures at which 5 wt% and 50 wt% decomposition occurs, $T_5$ and $T_{50}$, directly calculated from the TGA curves and $T_{max}$, the temperature at which the maximum rate of decomposition occurs, corresponding to the maximum of the first derivative of TGA curve are collected in the Table 3.1. As seen in the Figure 3.9, for the solution mixed composites, $T_{max}$ was shifted about 10°C upon addition of 1 wt% BDBA. The increase in the wt% of BDBA had no significant effect. For the composites involving 7 and 15 wt% BDBA, the shift was only about 12°C. However, PMMA composite with 15 wt% BDBA shows different decomposition behavior than the others. There is a second degradation step possibly resulted from the degradation of thermally stable boron networks.

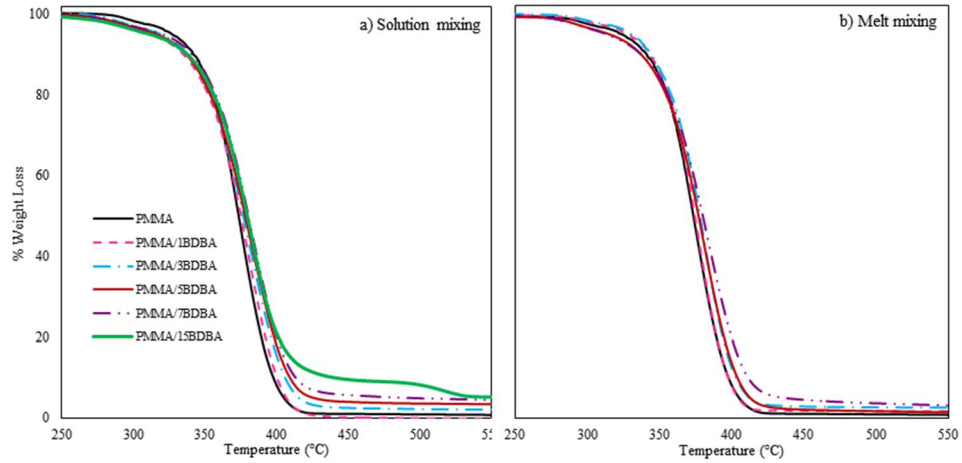


**Figure 3.8.** TGA curves of PMMA/BDBA composites prepared by solution and melt blending.

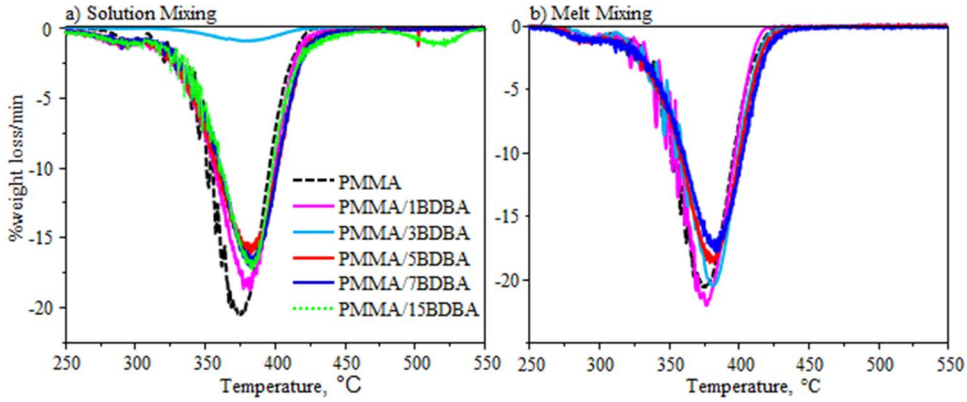


**Figure 3.9.** First derivative curves of TGA for PMMA/BDBA composites prepared by solution and melt blending

For the melt blended composites, as the amount of BDBA added was increased, thermal degradation of PMMA was shifted slightly to high temperature regions, especially the $T_{50}$ and $T_{max}$ values were increased. Upon addition of 1 wt% BDBA, $T_{max}$, was increased from 372.1°C to 377.7°C, indicating an increase of 5,6°C. For the composite involving 7 wt% BDBA about 12°C improvement was obtained. In

addition, for the melt blended composites char yields was lower than the corresponding values for the solution cast composites.

**Table 3.1.** TGA data of pure PMMA, its composites and nanocomposites prepared by solution and melt mixing.

| Compounds | | wt% BDBA | wt% C30B | $T_5$, °C | $T_{50}$, °C | $T_{max}$, °C | % Residue |
|---|---|---|---|---|---|---|---|
| PMMA | | | | 320.0 | 367.7 | 372.1 | 0 |
| Solution Mixed | PMMA/BDBA | 1 | | 311.5 | 374.0 | 382.5 | 0.05 |
| | | 3 | | 319.7 | 376.3 | 382.2 | 1.9 |
| | | 5 | | 317.5 | 378.0 | 383.5 | 3.1 |
| | | 7 | | 322.0 | 379.0 | 385.0 | 4.1 |
| | | 15 | | 312.5 | 380.0 | 384.0 | 5.0 |
| | PMMA/C30B/BDBA | | 3 | 337.0 | 381.7 | 389.1 | 4.9 |
| | | 1 | 3 | 296.7 | 375.0 | 383.5 | 1.0 |
| | | 3 | 3 | 326.3 | 381.0 | 389.1 | 4.7 |
| | | 5 | 3 | 324.7 | 381.5 | 386.3 | 3.0 |
| | | 7 | 3 | 269.8 | 376.2 | 382.8 | 2.9 |
| | | 15 | 3 | 326.5 | 382.1 | 389.1 | 6.3 |
| Melt Mixed | PMMA/BDBA | 1 | | 331.0 | 374.4 | 377.7 | 1.0 |
| | | 3 | | 333.5 | 377.5 | 382.6 | 2.5 |
| | | 5 | | 320.7 | 376.6 | 382.1 | 1.1 |
| | | 7 | | 318.0 | 380.0 | 384.0 | 2.6 |
| | PMMA/C30B/BDBA | | 3 | 341.0 | 383.8 | 388.8 | 4.0 |
| | | 1 | 3 | 335.3 | 380.0 | 385.0 | 4.1 |
| | | 3 | 3 | 327.0 | 383.0 | 389.7 | 3.3 |
| | | 5 | 3 | 330.3 | 383.4 | 390.1 | 3.8 |
| | | 7 | 3 | 328.8 | 382.8 | 390.0 | 3.9 |

### b) PMMA/C30B/BDBA Nanocomposites

Incorporation of Cloisite 30B into PMMA/BDBA composites promoted thermal stability of the polymer (Figure 3.10 and 3.11), $T_{max}$ was increased about 17°C

and the char formation was improved further because of the inorganic nature of the clay which can resist to high temperatures.. Although the thermal stability of PMMA was decreased upon incorporation of 1 wt% of BDBA into PMMA/C30B matrix, a slight improvement obtained as the amount BDBA added into the matrix was increased. However, the improvements in thermal stability of PMMA/C30B/BDBA nanocomposites cannot exceed that of PMMA/C30B for the solution mixed composites. For the melt blended composites a slight increase in thermal stability was achieved at high BDBA loadings, better thermal properties for the melt blended composites. Therefore, it can be said that melt mixing technique produces thermally more stable composites, starting to decompose especially at higher temperatures than solution mixing technique due to the dispersion of boron particles more uniformly.

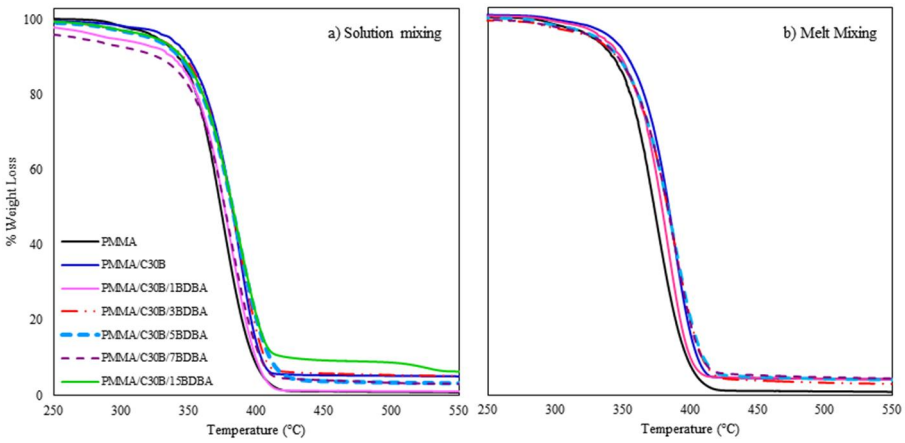


**Figure 3.10.** TGA curves of PMMA/C30B/BDBA nanocomposites prepared by solution and melt mixing

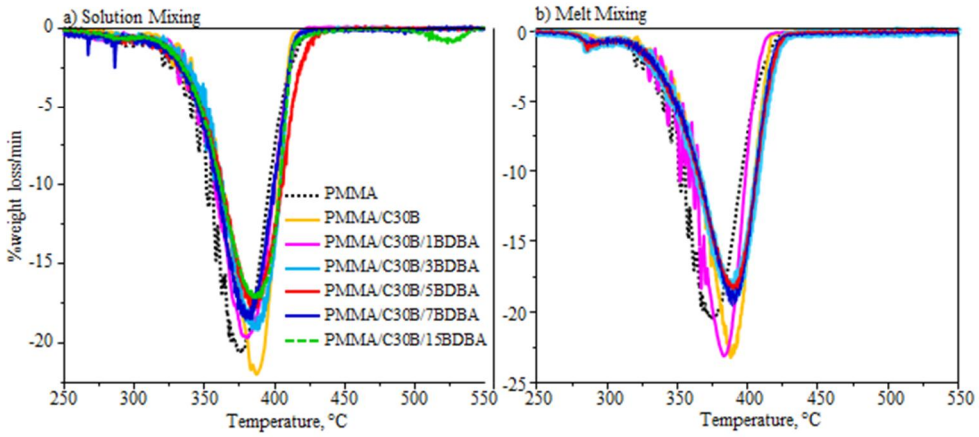


**Figure 3.11.** First derivative curves of TGA for PMMA/C30B/BDBA nanocomposites prepared by solution and melt blending

The TGA results indicated that both boron compounds and clay cause an increase in thermal stability of PMMA due to the barrier effects of these fillers which restrict the evaporation of small molecules during degradation of PMMA matrix. The enhancement in thermal degradation characteristics was more prominent for PMMA/C30B/BDBA nanocomposites, as the incorporation of clay together with the boron compound produces synergistic effects on the thermal stability of the polymer matrix.

### 3.2.2. Direct Pyrolysis Mass Spectrometry Analyses

The effects of boron compound on the thermal degradation of PMMA and its nanocomposites were also determined by the DP-MS technique. Pyrolysis mass spectrum of pure components, PMMA, BDBA, C30B and PMMA/BDBA and PMMA/C30B/BDBA composites involving different amounts of aromatic boronic acid were recorded as a function of temperature and analyzed systematically.

### 3.2.2.1. Pure Substances

#### a) PMMA

The total ion current, TIC, curve (the variation of total ion yield as a function of temperature), the pyrolysis mass spectrum recorded at the maximum of the TIC curve, at 381°C during the pyrolysis of PMMA are given in Figure 3.12.

The peak at m/z=100 Da is directly associated with MMA monomer resulted by the depolymerization mechanism during the thermal degradation of PMMA. The base peak (41 Da) is attributed with $C_3H_5$ fragment due to the dissociation of the monomer during ionization. Other intense peaks in the spectrum at 85, and 69 Da due to $C_3H_5CO_2$ and $C_3H_5CO$ are in accordance with the classical EI mass spectrum of methyl methacrylate. Moreover, weak peaks, 31 and 32 Da fragments which have peak maxima at the same temperature, are resulted from $CH_3O$ and $CH_3OH$ fragments. The weak peak in the TIC curve at around 308 °C is associated with the thermal degradation of low molar mass oligomers, elimination of unsaturated end groups and chains containing head to head linkages [46]. While the high temperature peak is attributed to products generated by mixture of unsaturated chain end (Scheme 1.4) and chain scission processes (Scheme 1.5) followed by depropagation step yielding mainly the monomer.

Single ion evolution profiles of these fragments show identical trends indicating that all the products were produced through the same decomposition pathways (Figure 3.12c). The relative intensities and the assignments made for the intense and/or characteristics peaks present in the pyrolysis mass spectrum of PMMA recorded at 381 °C are listed in Table 3.2.

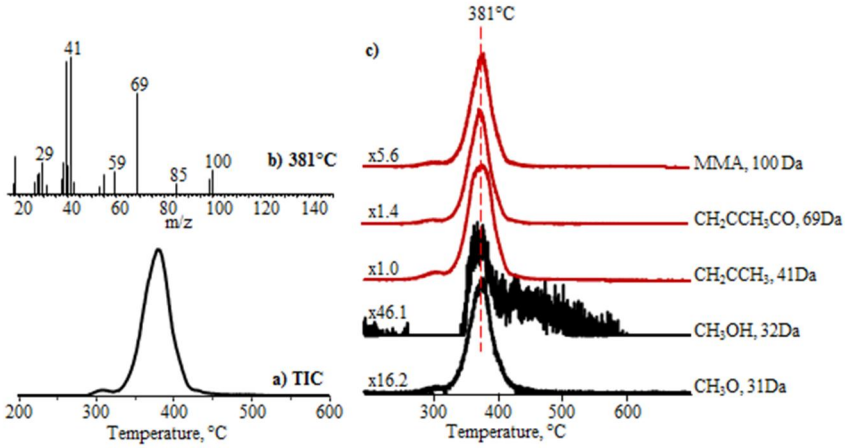


**Figure 3.12**. a) TIC curve, pyrolysis mass spectra of PMMA at b) 381 °C and c) Single ion evolution profiles of some selected products.

**Table 3.2.** Relative intensities and assignments made for the characteristic peaks recorded in the pyrolysis mass spectrum of PMMA at 381 °C

| m/z, Da | Relative Intensity | Assignments |
|---|---|---|
| 41 | 1000.0 | $C_3H_5$ |
| 69 | 716.4 | $C_3H_5CO$ |
| 85 | 747.0 | $C_3H_5COO$ |
| 100 | 178.3 | MMA, monomer |

**b) BDBA (1,4-benzenediboronic acid)**

The TIC curve and the pyrolysis mass spectrum at the maximum of the TIC curve, at 198°C recorded during the pyrolysis of BDBA are given in Figure 3.13. The molecular ion peak of BDBA is observed at 166 Da. The base peak at 45 Da can directly be associated with $B(OH)_2$ fragment ion. The assignments made for the most abundant peaks present in the pyrolysis mass spectrum at 198°C are collected in Table 3.3. The spectrum obtained is similar to the mass spectrum of BDBA given in NIST Mass Library.

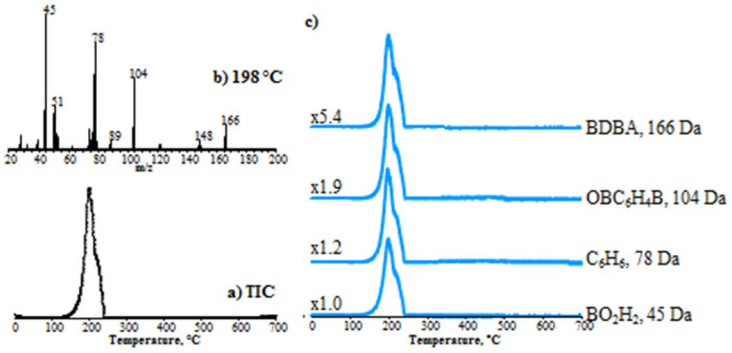


**Figure 3.13.** a. TIC curve, pyrolysis mass spectra of BDBA at b. 198 °C and c. Single ion evolution profiles of some selected products.

**Table 3.3.** Relative intensities and assignments made for the characteristic peaks recorded in the pyrolysis mass spectrum of BDBA at 198°C.

| m/z, Da | Relative Intensity | Assignments |
|---|---|---|
| 45 | 1000.0 | $B(OH)_2$ |
| 51 | 325.2 | $C_4H_3$ |
| 78 | 789.5 | $C_6H_6$ |
| 89 | 67.2 | $C_6H_5BH$ |
| 104 | 529.9 | $C_6H_5BO$ |
| 148 | 67.8 | $(BOH)_2C_6H_4BO$ |
| 166 | 181.9 | $(BOH)_2C_6H_4(BOH)_2$ |

### c) Cloisite 30B

Organically modified montmorillonite, Cloisite 30B, was analyzed by DP-MS and Figure 3.14 shows the TIC curve and pyrolysis mass spectra at the maxima of the two overlapping peaks present in the TIC curve. In the mass spectrum recorded at 286 °C, the base peak is at 88 Da due to $CH_3N(CH_2)C_2H_4OH$ fragment resulted from classical fragmentation mechanism of amines. Other intense low mass peaks at 28,44 and 58 Da are associated with $C_2H_4$, $C_2H_4NH_2$, $C_3H_6NH_2$ fragments respectively. The high mass peaks at 268 Da is assigned to

$C_{16}H_{33}(CH_3)NCH_2$, and/or $CH_3N(C_{14}H_{26})C_2H_4OH$ fragment and the one at 296 Da is attributed to $C_{18}H_{37}(CH_3)NCH_2$, and/or $CH_3N(C_{16}H_{30})C_2H_4OH$ fragments. At high temperatures, at around 425 °C, a different fragmentation pattern is seen and related to degradation of high molar mass hydrocarbons. Table 3.4 shows the intensities and the assignments of C30B fragments at two different temperatures.

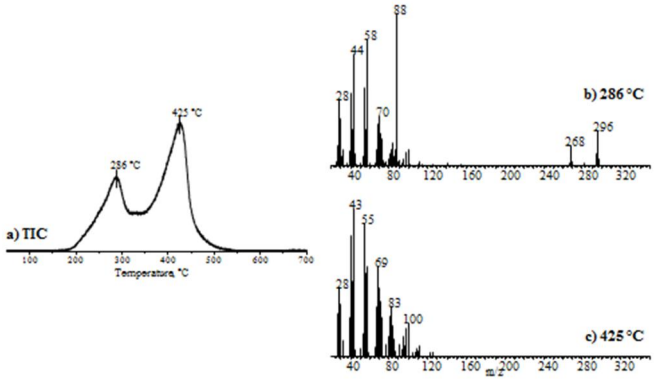


**Figure 3.14.** a) TIC curve and pyrolysis mass spectra of Cloisite 30B recorded at b) 286 °C and c) 425°C.

**Table 3.4.** Relative intensities and assignments made for the characteristic peaks recorded in the pyrolysis mass spectrum of Cloisite 30B at 286°C and 425°C.

| m/z, Da | Relative Intensity | | Assignments |
|---|---|---|---|
| | 286 °C | 425 °C | |
| 43 | 618.4 | 1000.0 | $C_3H_7$ |
| 55 | 485.5 | 942.7 | $C_4H_7$ |
| 58 | 826.3 | 432.5 | $C_3H_6NH_2$ |
| 69 | 271.2 | 619.3 | $C_5H_9$ |
| 88 | 1000.0 | 10.5 | $CH_3N(CH_2)C_2H_4OH$ |
| 268 | 134.4 | 2.9 | $C_{16}H_{33}N(CH_3)_2$ |
| 296 | 222.5 | 1.1 | $C_{18}H_{37}(CH_3)NHCH_2$ and/or $C_{19}H_{38}NO$ |

### 3.2.2.2. PMMA/BDBA Composites

The direct pyrolysis mass spectrometry analyses of PMMA/BDBA composites at various BDBA contents prepared by solution mixing and melt blending were performed to investigate the effects of amount of boron compound and mixing method on thermal degradation behavior and product distribution.

#### a) PMMA/BDBA composites prepared by solution casting

The TIC curves of PMMA and PMMA/BDBA composites involving 1, 3, 5, 7 and 15 wt% BDBA prepared by solution mixing are given in Figure 3.15. It can be observed from the figure that the TIC curves are shifted slightly to high temperature regions as the wt% of BDBA present in the composite increases, indicating an improvement in the thermal stability upon incorporation of BDBA into PMMA matrix. Furthermore, a weak shoulder at around 480°C is appeared in the TIC curves. In addition, a very weak peak at around 650 °C is noticed for the composites involving 5, 7 and 15 wt% BDBA.

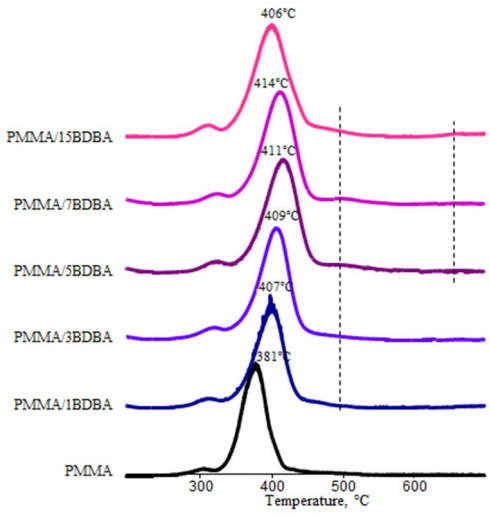


**Figure 3.15.** TIC curves of PMMA/BDBA composites involving 1, 3, 5, 7 and 15 wt% BDBA prepared by solution mixing.

In Figure 3.16, the TIC curve, and the pyrolysis mass spectra of PMMA/BDBA containing 15 wt% BDBA recorded at 406 °C and 650 °C are shown as a representative example. At 406 °C, the characteristic peaks at 41, 69 and 100 Da, due to the fragments $C_3H_5$ and $C_3H_5CO$ and MMA respectively, are detected indicating that the thermal decomposition of PMMA took place via depolymerization mechanism yielding mainly the monomer, in accordance with the well-known thermal decomposition mechanism. However, the relative intensity of the monomer peak is diminished slightly. The pyrolysis mass spectra recorded at around 439°C are also dominated with almost identical peaks, yet, weak peaks that can be associated with products generated by trans-esterification reaction between the ester groups of PMMA and the hydroxyl group of the boronic acid, such as peak at 32 Da attributed to evolution of $CH_3OH$, are detectable. The peaks at 77, 104 and 312 Da in the mass spectrum recorded at around 650 °C can directly be associated with $C_6H_5$, $C_6H_5BO$ and triphenyl borozin, $(C_6H_5BO)_3$ respectively indicating decomposition of an aromatic boron network (Figure 3.16.d). The formulas of the fragments involving B atom are confirmed by using isotopic peaks of B.

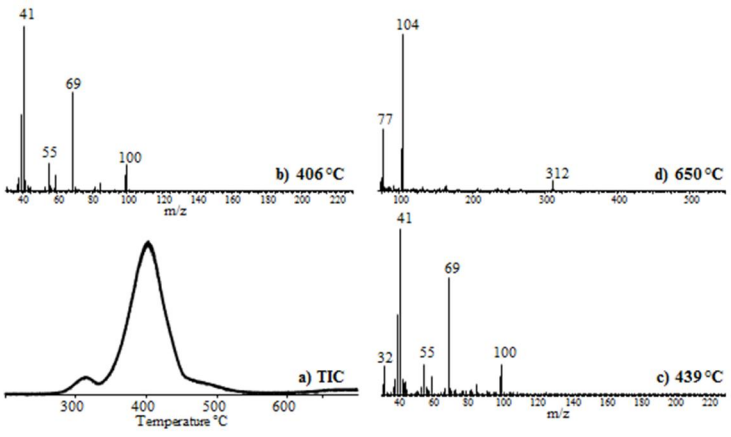


**Figure 3.16.** a) TIC curve of PMMA/BDBA involving 15 wt% BDBA and pyrolysis mass spectra recorded at b) 406, c) 439 and d) 650°C.

Single ion evolution profiles of intense and characteristic products, such as $C_3H_5$ (41 Da), $C_3H_5CO$ (69 Da), MMA (100 Da) and $CH_3O$ (31 Da) due to decomposition of PMMA, $CH_3OH$ (32 Da) and $C_3H_5CO_2B(OH)C_6H_4$ (189 Da) generated by trans-esterification reaction between BDBA and PMMA, BDBA (166 Da), $C_6H_5$ (77 Da), $OBC_6H_4$ (104 Da) diagnostic for BDBA and $(C_6H_5BO)_3$ (312 Da) associated with a network structure recorded during the pyrolysis of PMMA/BDBA involving 15 wt% BDBA are given in Figure 3.17. As can be noted from the figure, the diagnostic fragments of MMA, $C_3H_5$ (41 Da), $C_3H_5CO$ (69 Da), and MMA (100 Da) have identical evolution profiles reaching maximum yield at around 406 °C. The single ion evolution profile of the fragment $CH_3O$ (31 Da) also show maximum at 406°C, however, a shoulder at around 439 °C, at the maximum of the evolution profile of $CH_3OH$ (32 Da) is also present. Actually, elimination of 32 Da product, due to $CH_3OH$ and/or $O_2$ is also detected during the pyrolysis of neat PMMA, but its evolution profile is identical to all other diagnostic degradation products of the polymer. Thus, it may be concluded that the elimination of $CH_3O$ occurs from two different sources; by the dissociation of MMA at around 406 °C and by dissociation of $CH_3OH$ due to the reaction of boron compound with ester groups at around 439 °C.

The trans-esterification reaction as shown in Scheme 3.1, yields $CH_3OH$ and methacrylate units linked to aromatic boron compounds. The evolution profile of $C_3H_5CO_2B(OH)C_6H_4$ (189 Da) given in the figure, shows a weak peak in the same region confirming trans-esterification reaction between BDBA and ester groups of PMMA.

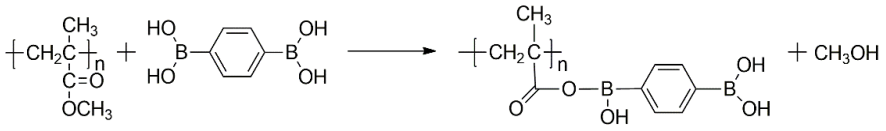


**Scheme 3.1.** Trans-esterification reaction between PMMA and benzene-1,4-diboronic acid

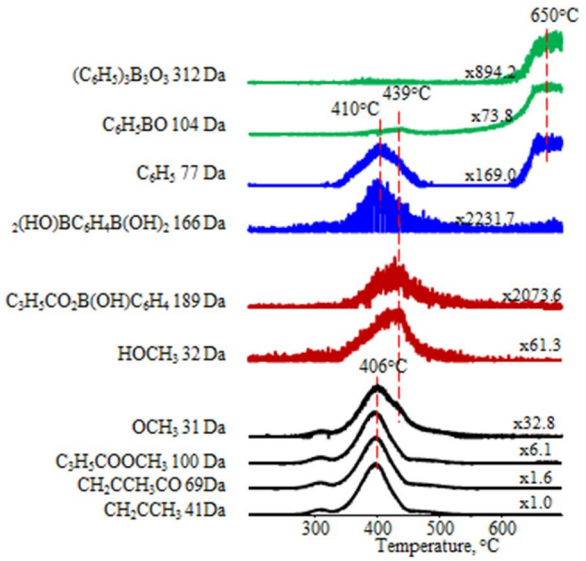


**Figure 3.17.** Single ion evolution profiles of some selected products recorded during the pyrolysis of PMMA/BDBA involving 15 wt% BDBA.

The relative yields of the characteristic degradation products of BDBA, such as BDBA (166 Da), $C_6H_5$ (77 Da), and $OBC_6H_4$ (104 Da) are also quite weak and variations in their evolution profiles are noted. The molecular ion shows a single peak in its pyrogram with a maximum at around 410 °C, significantly higher than the corresponding value recorded for pure BDBA, (198 °C). The loss of BDBA, at significantly higher temperatures, suggests strong interactions between BDBA and the polymer matrix and/or generation of a network structure. The pyrograms of $C_6H_5$ (77 Da), and $OBC_6H_4$ (104 Da) show two peaks, a weak peak at around 410 °C and a stronger one at around 650°C. On the other hand, the evolution of triphenyl borozin, $(C_6H_5BO)_3$ is only detected at around 650°C. The losses of BDBA and diagnostic fragments of BDBA at around 410°C suggest decomposition of chains generated by trans-esterification reactions, whereas, evolution of triphenyl borozin at elevated temperatures confirms the generation of a boron network structure.

In order to clarify the effect of wt% of BDBA on extent of trans-esterification reactions and generation of the network structure, pyrolysis mass spectra of PMMA/BDBA composites with various BDBA contents were analyzed in details. In Figure 3.18, single ion evolution profiles of diagnostic products of PMMA, $C_3H_5$ (41 Da), products associated with trans-esterification reactions between BDBA and PMMA (32 Da) and $OBC_6H_5$ (104 Da) and triphenyl borozin (312 Da) recorded during the pyrolysis of PMMA and PMMA/BDBA composites involving 1, 3, 5, 7 and 15 wt% BDBA are depicted.

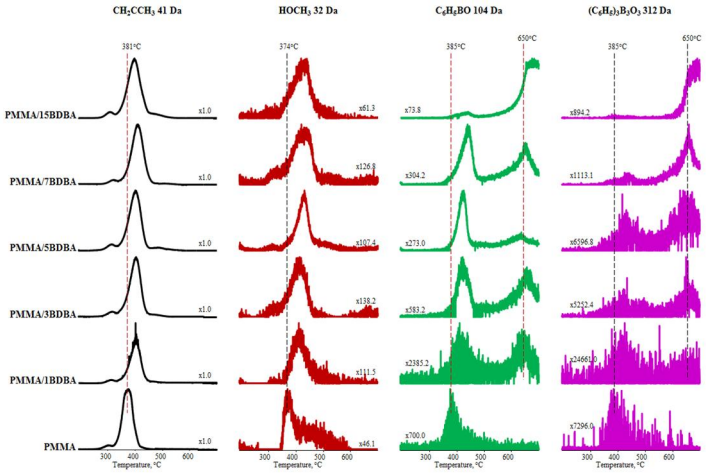


**Figure 3.18.** Single ion evolution profiles of some selected products recorded during the pyrolysis of pure PMMA and PMMA/BDBA involving 1, 3, 5, 7 and 15 wt% BDBA.

In general, as the amount of BDBA incorporated into PMMA is increased the single ion pyrograms shifts to higher temperatures. In addition, the relative abundances of $CH_3OH$ lost above 439°C and those of the products associated with decomposition of a boron network, such as $C_6H_5BO$ and $(C_6H_5BO)_3$ lost around 650°C are enhanced noticeably. Similarly, the relative yield of $C_6H_5BO$ at around 439°C is increased supporting the increase in the extent of the trans-

esterification reactions. The trends in the single ion evolution profiles and the presence of isotopic peaks of boron confirmed the generation of a network structure when the wt% of BDBA was greater or equal to 3.

**b) PMMA/BDBA composites prepared by melt blending**

The TIC curves of PMMA and PMMA/BDBA composites prepared by melt blending involving 1, 3, 5 and 7 wt% BDBA are given in Figure 3.19. Again, the TIC curves are shifted slightly to high temperature regions as the wt% of BDBA present in the composite increases. However, the improvement in the thermal stability is slightly smaller than the corresponding composites prepared by solution mixing. In addition, unlike what was observed for the solution casted composites, the TIC curves show no high temperature shoulder or peak. As the amount of BDBA added into the polymer matrix increases, the intense peak corresponding to main decomposition is broadened.

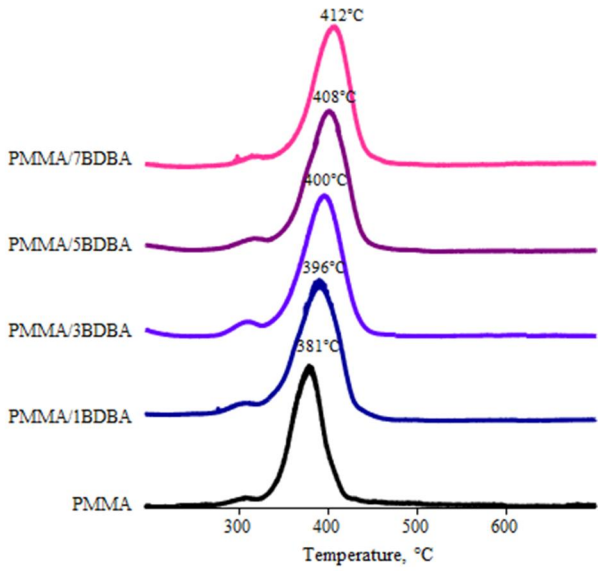


**Figure 3.19.** TIC curves of PMMA/BDBA composites prepared by melt blending involving 1, 3, 5 and 7 wt% BDBA.

In Figure 3.20, the TIC curve, and the pyrolysis mass spectrum of PMMA/BDBA containing 7 wt% BDBA recorded at 412 °C are shown as a representative example. Again, the mass spectrum is dominated with diagnostic fragments of MMA, yet, the decrease in the relative intensity of the monomer peak is more pronounced. In addition, the peaks associated with the products diagnostic to degradation of units generated by trans-esterification reactions are more intense than the corresponding ones detected during the pyrolysis of the composites prepared by solution casting. However, no peak that can be related to elimination of fragments due to decomposition of a boron network is detected.

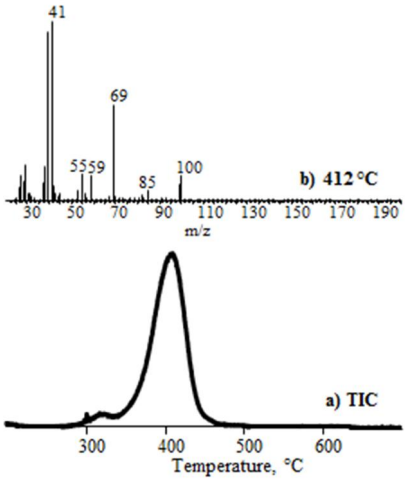


**Figure 3.20.** a) TIC curve of PMMA/BDBA prepared by melt blending, involving 7 wt% BDBA and b) pyrolysis mass spectrum recorded at 412°C.

In Figure 3.21, the single ion evolution profiles of $C_3H_5$ (41 Da), $C_3H_5CO$ (69 Da), MMA (100 Da) and $CH_3O$ (31 Da) due to decomposition of PMMA, $CH_3OH$ (32 Da) and $C_3H_5CO_2B(OH)C_6H_4$ (189 Da) generated by trans-esterification reaction between BDBA and PMMA, BDBA (166 Da), $C_6H_5$ (77 Da), $OBC_6H_4$ (104 Da) diagnostic for BDBA and $(C_6H_5BO)_3$ (312 Da) associated with a network structure recorded during the pyrolysis of

PMMA/BDBA prepared by melt blending, involving 7 wt% BDBA are given. The trends in the evolution profiles clearly indicate that a boron network structure is not generated. The products that can be associated with decomposition of units formed by trans-esterification reactions are maximized at around 428°C, at lower temperatures than the corresponding ones eliminated during the pyrolysis of the solution mixed composites. However, their abundances are enhanced noticeably. In addition, for this sample, all the products associated with the decomposition of boron involving products showed identical trends.

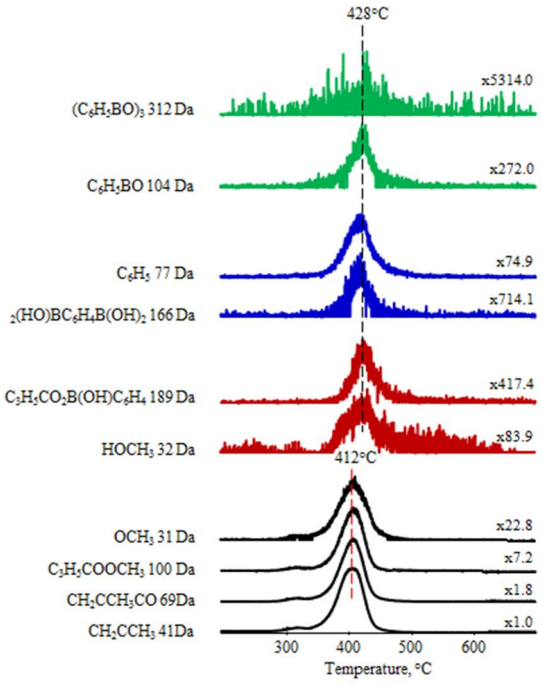


**Figure 3.21.** Single ion evolution profiles of some selected products recorded during the pyrolysis of PMMA/BDBA involving 7 wt% BDBA prepared by melt blending.

In Figure 3.22, the single ion evolution profiles of diagnostic products of PMMA, $C_3H_5$ (41 Da), products associated with trans-esterification reactions between BDBA and PMMA (32 Da), $OBC_6H_4$ (104 Da) and triphenyl borozin

(312 Da) detected during the pyrolysis of melt blended PMMA/BDBA composites are shown.

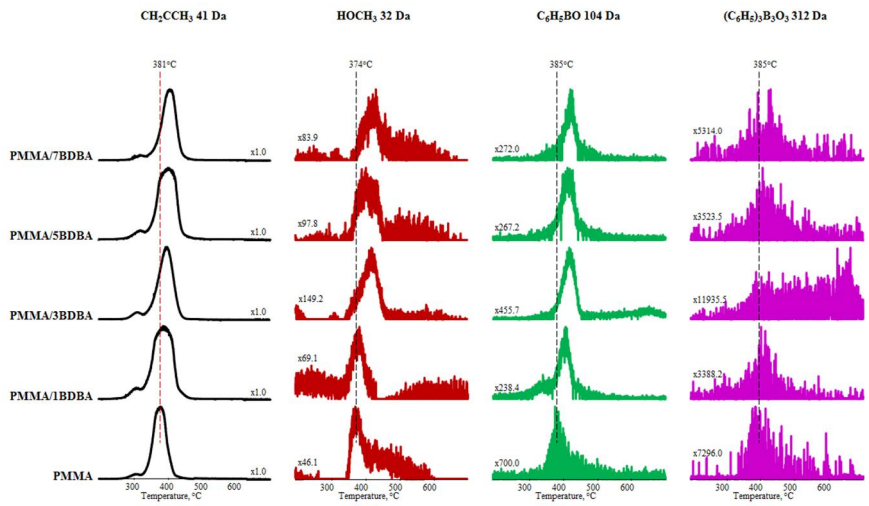


**Figure 3.22.** Single ion evolution profiles of some selected products recorded during the pyrolysis of PMMA/BDBA prepared by melt blending involving 1, 3, 5, 7 wt% BDBA.

In general, as the amount of BDBA incorporated into PMMA is increased the single ion pyrograms shifts to higher temperatures. In addition, the relative abundances of $CH_3OH$ and $C_3H_5CO_2B(OH)C_6H_4$ (189 Da) lost around 428°C are enhanced noticeably. It may be proposed that as the amount of BDBA is increased the extent of trans-esterification reactions is also increased.

It may further be suggested that, during the melt blending, BDBA molecules are homogenously distributed in the polymer matrix which promotes trans-esterification reactions but inhibits generation of a network structure. On the other hand, in the case of solution mixing, BDBA molecules are accumulated leading to a boron network structure that decomposes at elevated temperatures in accordance with SEM results. Considering the significantly higher thermal

stability of the units generated by trans-esterification reactions for the solution casted composites, formation of a network structure at least to a certain extent may also be proposed for the boronic acid units reacted with MMA ester groups. The loss of BDBA at significantly higher temperatures than the evaporation temperature of pure BDBA supports this proposal.

#### 3.2.2.3. PMMA/C30B/BDBA Nanocomposites

The TIC curves of PMMA and PMMA/C30B nanocomposites prepared by melt blending and solution casting involving 3wt% Cloisite 30B, are shown in Figure 3.23. The TIC curves are shifted slightly to high temperature regions upon incorporation of nanoclay into polymer matrix prepared by both techniques. The broad peak in the TIC curve of PMMA becomes narrower in the presence of nanoclay. Yet, a shoulder at around 430°C in the TIC curve of the melt blended sample, whereas a weak peak at around 437°C in that of the solution casted sample are appeared. On the other hand, the mass spectra recorded at the peak maxima and at the shoulder are almost identical with the corresponding one for PMMA, indicating that the presence of nanoclay in the matrix does not affect the mechanism of thermal degradation of PMMA.

The high temperature shoulder is quite abundant for the melt blended composite, however, appears at a lower temperature than the corresponding weak peak detected in the TIC curve of the solution casted composite, for which, the TEM results indicated a better dispersion of clay. It may be thought that the decomposition of PMMA chains intercalated into the clay galleries occurs at higher temperatures.

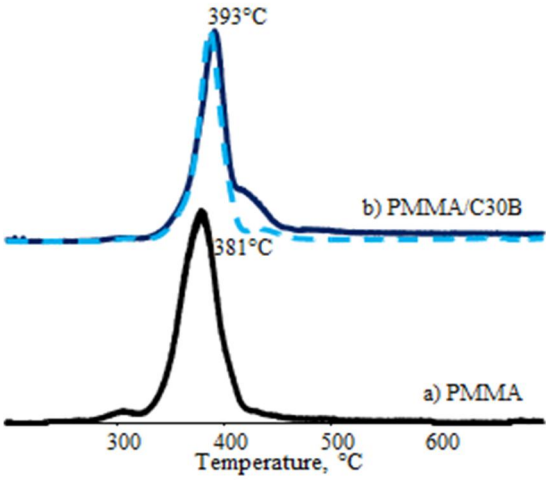


**Figure 3.23.** a) TIC curves of PMMA and PMMA/C30B nanocomposites prepared by melt blending (solid line) and solution casting (dashed line).

**a) PMMA/BDBA nanocomposites prepared by solution casting**

The TIC curves of PMMA/C30B and PMMA/C30B/BDBA nanocomposites involving 1, 3, 5, 7 and 15 wt% BDBA prepared by solution mixing are given in Figure 3.24. The TIC curves of the corresponding composites involving only BDBA in the PMMA matrix are also included as dotted lines for comparison. It can be observed from the figure that upon incorporation of Cloisite 30B, the decomposition of PMMA is shifted slightly to high temperature regions, and is completed in a narrower temperature range. Furthermore, the weak shoulder at around 440°C and the weak peak at around 650°C are disappeared.

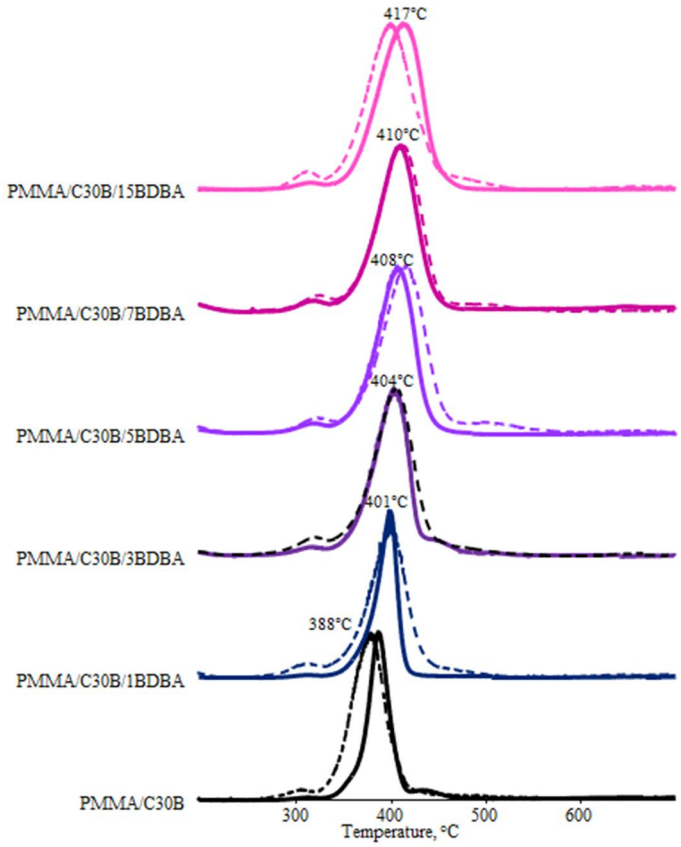


**Figure 3.24.** TIC curves of PMMA/BDBA composites prepared by solution casting involving 1, 3, 5, 7 and 15 wt% BDBA and 3 wt% C30B (dashed line for composites containing only BDBA and temperatures belong to the PMMA/C30B/BDBA).

In Figure 3.25, the TIC curve, and the pyrolysis mass spectrum of PMMA/C30B/BDBA containing 15 wt% BDBA recorded at 417 °C are predicted. The mass spectrum at 417°C is again dominated with diagnostic fragments peaks of MMA.

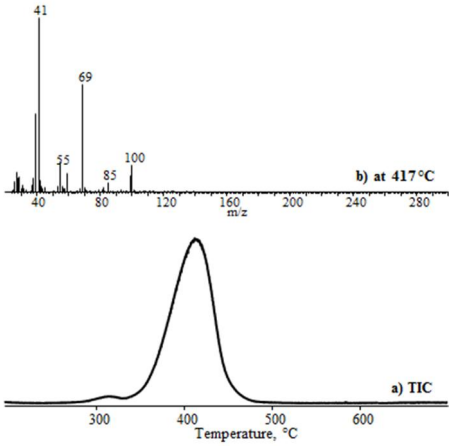


**Figure 3.25.** a) TIC curve of PMMA/BDBA prepared by solution casting, involving 15 wt% BDBA and 3 wt% C30B and b) pyrolysis mass spectrum recorded at 417°C.

The single ion evolution profiles of the representative pyrolysis products $C_3H_5$ (41 Da), $C_3H_5CO$ (69 Da), MMA (100 Da) and $CH_3O$ (31 Da) due to decomposition of PMMA, $CH_3OH$ (32 Da) and $C_3H_5CO_2B(OH)C_6H_4$ (189 Da) generated by trans-esterification reaction between BDBA and PMMA, BDBA (166 Da), $C_6H_5$ (77 Da), $OBC_6H_4$ (104 Da) diagnostic for BDBA and $(C_6H_5BO)_3$ (312 Da) associated with a network structure recorded during the pyrolysis of PMMA/BDBA prepared by solution casting involving 15 wt% BDBA are shown in Figure 3.26. The corresponding ones recorded during the pyrolysis of the composites containing only BDBA as additive are also included in the figure for comparison. It can be noticed from the figure that no significant change is detected in the temperature ranges of thermal degradation of PMMA/BDBA composite upon incorporation of 3 wt% C30B. However, increase in the relative yields of the products due to decomposition of units generated by trans-esterification reactions is detected. These products are maximized at around 437°C, at slightly lower temperatures than that was recorded for the composites involving only BDBA as an additive. On the other hand, the products associated with decomposition boron network almost totally disappeared.

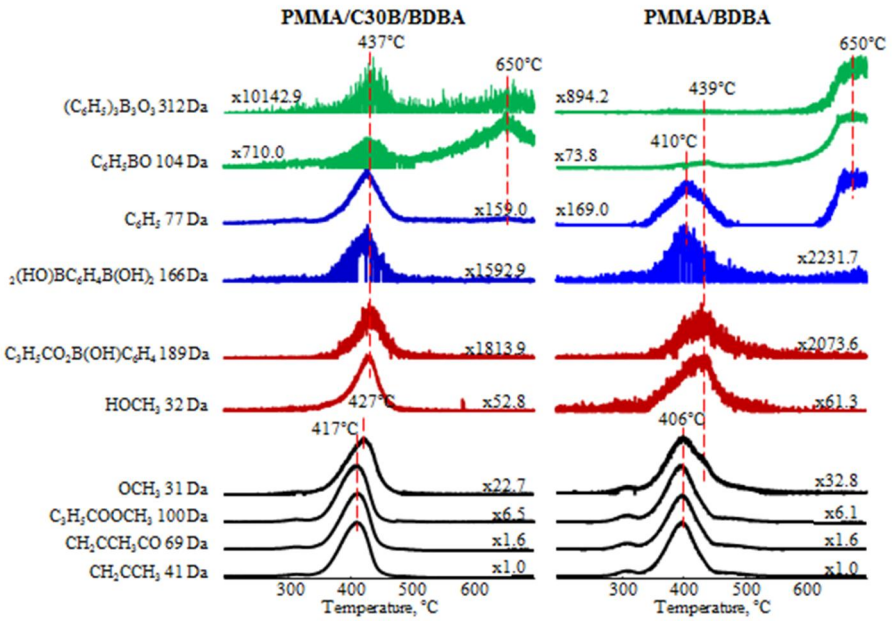


**Figure 3.26.** Single ion evolution profiles of some selected products recorded during the pyrolysis of PMMA/C30B/BDBA prepared by solution casting, involving 15 wt% BDBA and 3 wt% C30B.

The single ion evolution profiles of diagnostic products of PMMA, $C_3H_5$ (41 Da), product associated with trans-esterification reactions between BDBA and PMMA (32 Da) and $C_6H_5BO$ (104 Da) detected during the pyrolysis of PMMA/C30B/BDBA nanocomposites involving 1, 3, 5, 7 and 15 wt% BDBA are given in Figure 3.27. It is clear that the evolution profiles of all products shift slightly to high temperatures as the amount of BDBA added into PMMA matrix increases. In the presence of OMMT, the relative yields of products associated with the units generated by trans-esterification reactions are increased while those attributed to decomposition of boron network are decreased. It may be thought that in the presence of nanoclay, accumulation of aromatic boronic acid yielding network structures that decompose at elevated temperatures is less probable.

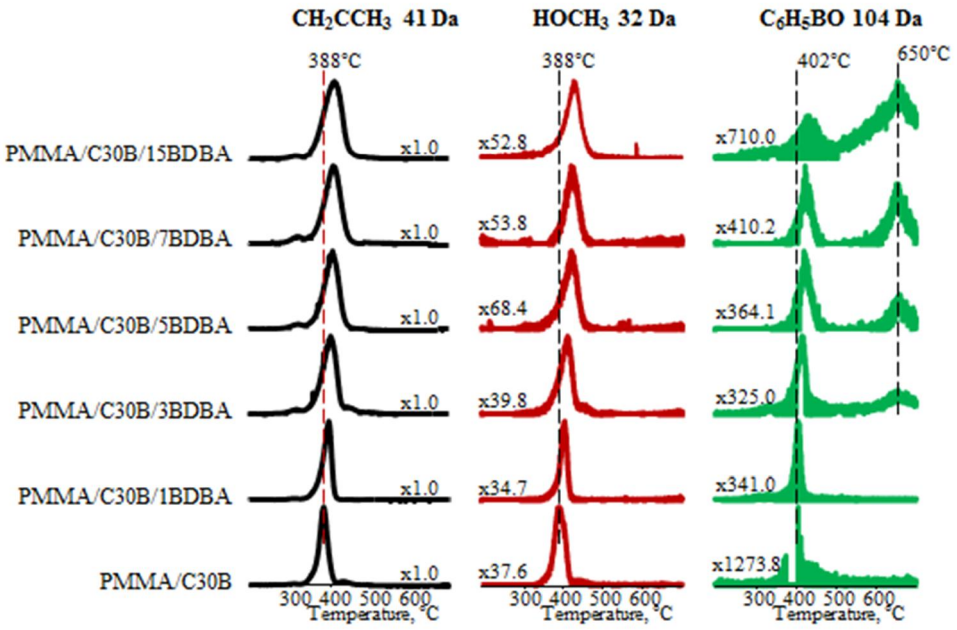


**Figure 3.27.** Single ion evolution profiles of some selected products recorded during the pyrolysis of PMMA/BDBA prepared by solution casting involving 1, 3, 5, 7 and 15 wt% BDBA and 3 wt% C30B.

**b) PMMA/BDBA nanocomposites prepared by melt blending**

In Figure 3.28, the TIC curves of PMMA/C30B and PMMA/C30B/BDBA nanocomposites involving 1, 3, 5 and 7 wt% BDBA prepared by melt mixing are shown. Again, the TIC curves of the corresponding composites involving only BDBA in the PMMA matrix are also included as dotted lines for comparison. Upon incorporation of OMMT into PMMA matrix, the decomposition of PMMA is shifted slightly to high temperature regions, and is completed in a narrower temperature range.

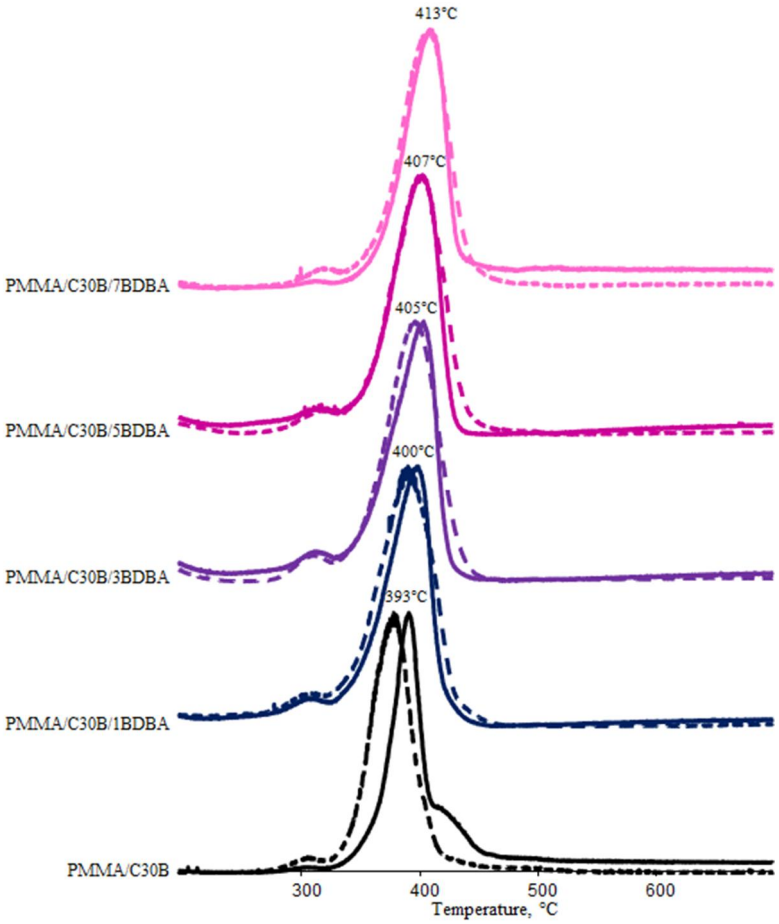


**Figure 3.28.** TIC curves of PMMA/BDBA composites prepared by melt blending involving 1, 3, 5 and 7 wt% BDBA and 3 wt% C30B (dashed line for composites containing only BDBA and temperatures belong to the PMMA/C30B/BDBA).

In Figure 3.29, the TIC curve, and the pyrolysis mass spectrum of PMMA/C30B/BDBA containing 7 wt% BDBA recorded at 413 °C are predicted. The mass spectrum at 413°C is again dominated with diagnostic fragments of MMA.

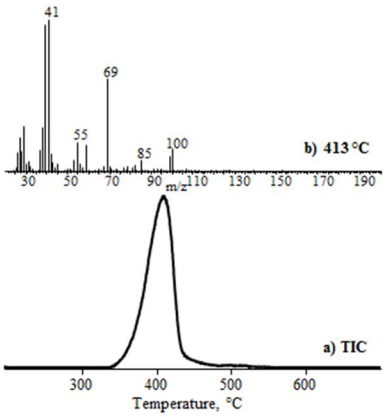


**Figure 3.29.** a) TIC curve of PMMA/BDBA prepared by melt blending, involving 7 wt% BDBA and 3 wt% C30B and b) pyrolysis mass spectrum recorded at 413°C.

In Figure 3.30, the single ion evolution profiles of representative pyrolysis products recorded during the pyrolysis of PMMA/C30B/BDBA prepared by melt blending involving 7 wt% BDBA are depicted. For comparison, the corresponding ones detected during the pyrolysis of the composites containing only BDBA as additive are again included in the figure. The thermal degradation of PMMA occurs almost in the same temperature region, whereas, elimination of fragments indicating decomposition of units generated by trans-esterification reactions takes place at slightly higher temperatures upon incorporation of 3 wt% C30B. In addition, the relative yields of products due to decomposition of units generated by trans-esterification reactions are increased.

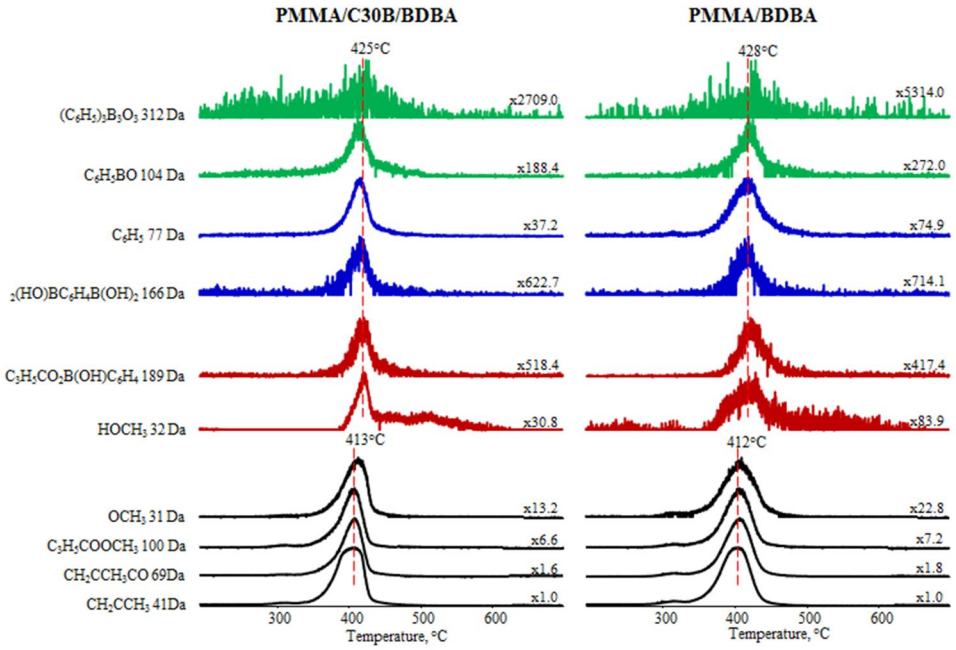


**Figure 3.30.** Single ion evolution profiles of some selected products recorded during the pyrolysis of PMMA/BDBA involving 7 wt% BDBA and 3 wt% C30B prepared by melt blending.

The single ion evolution profiles of diagnostic products of PMMA, $C_3H_5$ (41 Da), product associated with trans-esterification reactions between BDBA and PMMA (32 Da) and $C_6H_5BO$ (104 Da) fragment detected during the pyrolysis of PMMA/C30B/BDBA nanocomposites involving 1, 3, 5 and 7 wt% BDBA are given in Figure 3.31. Again, the evolution profiles of all the products shifted slightly to high temperatures with the increased amount of BDBA added into PMMA matrix.

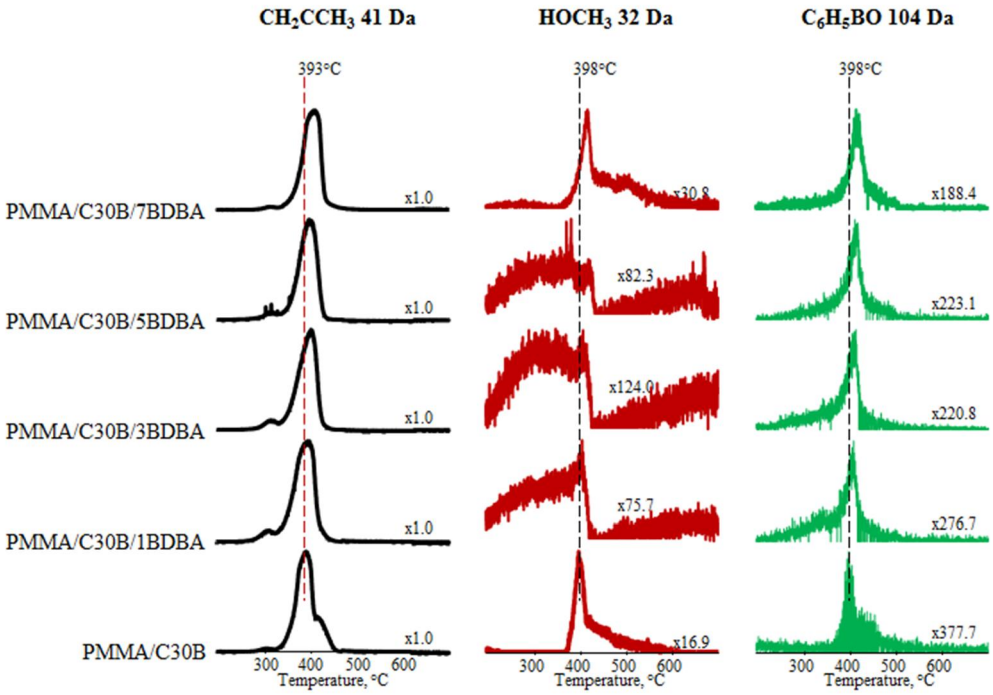


**Figure 3.31.** Single ion evolution profiles of some selected products recorded during the pyrolysis of PMMA/BDBA prepared by melt blending involving 1, 3, 5 and 7 wt% BDBA and 3 wt% C30B.

In Figure 3.32, the TIC curves of neat PMMA and PMMA/C30B nanocomposites and PMMA/BDBA composites involving 7 wt% BDBA and PMMA/C30B/BDBA nanocomposites prepared by two techniques are shown for a general comparison. It is clear that the thermal stability increases in the presence of both OMMT and BDBA, yet the effect of BDBA is more pronounced. Contrary, to the trends observed for PMMA/C30B nanocomposite, thermal decomposition of the composites involving BDBA is completed in a broader temperature region compared to neat PMMA. The effect of OMMT on thermal stability of PMMA/BDBA composites prepared by both techniques is almost negligible. Yet, as discussed before, the interactions of boron compound with ester groups of PMMA are enhanced while the generation of a network structure is inhibited in the presence of OMMT.

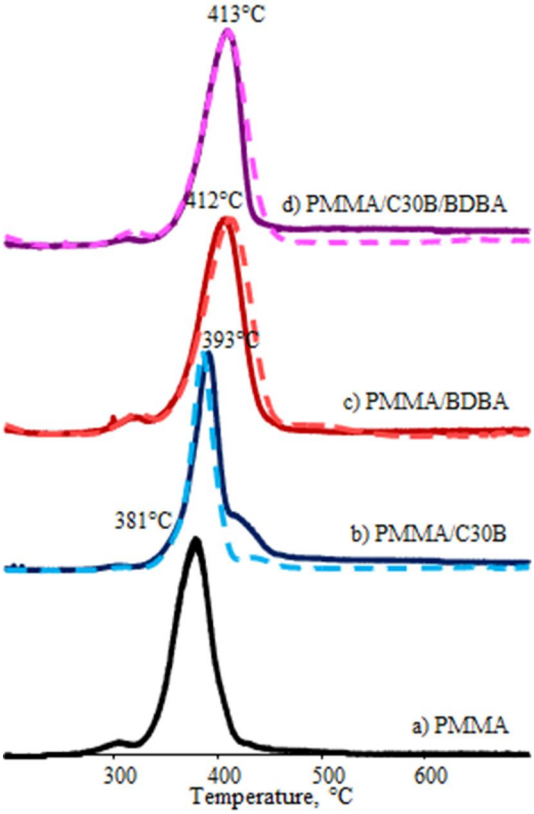


**Figure 3.32.** TIC curves recorded during the pyrolysis of PMMA, and PMMA/C30B, c) PMMA/BDBA and d) PMMA/C30B/BDBA composites prepared by solution mixing (dashed line) and melt blending (solid line).

In Figure 3.33, variations of the temperature at which the yields of $C_3H_5$ and $CH_3OH$ are maximized as a function of BDBA content are depicted. It can be observed from the figure that the temperature is increased noticeably upon incorporation of BDBA and OMMT. As the amount of BDBA increases the peak maximum shifts to high temperature regions. The increase in thermal stability of PMMA chains is greatest for the PMMA/BDBA composites prepared by solution mixing. In the presence of OMMT, the effect of mixing technique is almost negligible. Contrary to the general trends, for the PMMA/BDBA composite involving 15 wt% BDBA prepared by solution mixing, the temperature at which the yield of $C_3H_5$ and $CH_3OH$ is maximized is decreased

noticeably. It may be thought that at high loadings, as the probability of generation of a boron network increases inhibiting the interactions between BDBA and ester groups of PMMA, thus, limiting the improvement in thermal stability.

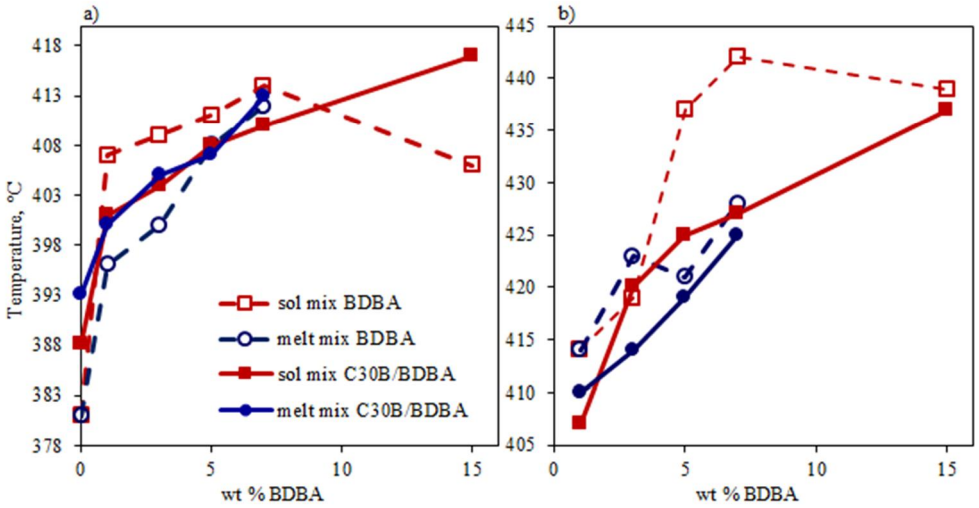


**Figure 3.33.** Variations of the temperature at which the yields of a) $C_3H_5$ and b) $CH_3OH$ are maximized as a function of BDBA content

### 3.3. Flammability Tests

UL-94V and LOI tests were used to analyze flame characteristics of PMMA and its nanocomposites. Flame tests were only performed for the melt mixed nanocomposites and the solution mixed PMMA/C30B involving 15 wt% BDBA.

#### 3.3.1. UL-94V Ratings

Dripping was seen when the pure PMMA was burned. With the addition of the boronic acid and clay, composites were burned to clamp without dripping. As mentioned before, Morgan et al. suggested that during combustion, boronic acid produces glassy network structure which inhibits flame growth and promotes

char formations [15]. Using benzene-1,4-diboronic acid increased burning periods of the compounds producing a thick char layer. This char formation may indicate the generation of a network structure, however, as burning of all the composites were completed in about 30 seconds, it can be concluded that BDBA up to 15 wt% is not an adequate flame retardant for PMMA according to UL-94V test standards.

Similarly, clay acted as a protective layer by producing char layer on the surface of PMMA but still incorporation of OMMT with BDBA and PMMA matrix did not cause further improvement in burning time or reduction in burning rate. Therefore, it is difficult to classify of all these material according to UL-94V test standards.

### 3.3.2. LOI Ratings

Oxygen index was used to evaluate the ease of extinction of compounds. The minimum percentage of oxygen to sustain combustion of an ignited specimen was measured for PMMA/BDBA and PMMA/C30B/BDBA nanocomposites and results are illustrated in Figure 3.34. The minimum amount of oxygen needed for the ignition of pure PMMA was 18.1%. This value was improved slightly as the amount of boron compound incorporated was increased. For PMMA/BDBA composites, the greatest enhancement was obtained upon the addition of 7 wt% boron compound. Addition of 15 wt% boron compound caused a slight increase in LOI value. When OMMT was added to PMMA matrix, LOI value was enhanced from 18.1% to 18.4% indicating that the ignition characteristic was affected by the presence of clay. The enhancement in the oxygen index was continued upon incorporation of the boron compounds into PMMA/C30B matrix. For the nanocomposite involving 15 wt% BDBA, LOI value was determined as 18.8%. This small increase may be resulted from the synergistic effects of clay and boron compounds.

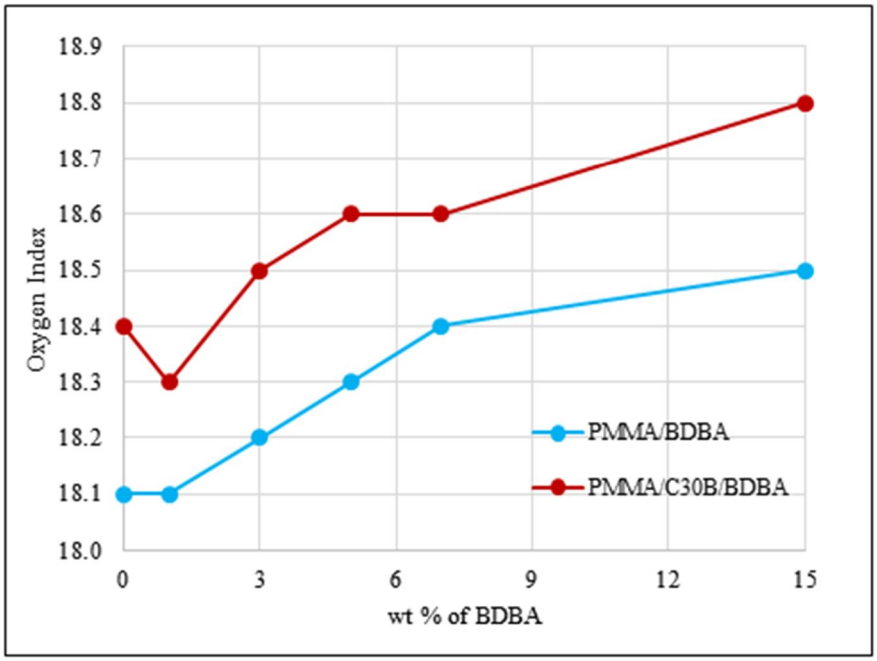


**Figure 3.34.** LOI values of PMMA/BDBA composites and PMMA/C30B/BDBA nanocomposites as a function of BDBA content.

As oxygen indices of nanocomposites show only very small improvement, the additives with selected amounts cannot be classified as flame retardant materials for PMMA. Real flame retardancy can only be obtained when the LOI values are greater than 25%. Below this amount, material is easily ignited and not easily extinguished once it is ignited as in case of our study. This failure may be due to several reasons. One possibility is that the interactions between PMMA and boron compound was not constructed very effectively to create a glassy network structure which can inhibit the burning of the sample. Another possibility is related to the dispersion of nanoclay in the PMMA matrix, the extent of exfoliated structure may be limited. Furthermore, the amount of fillers, especially the boron compound, may be insufficient to improve flame retardant characteristics of PMMA.

### 3.4. Mechanical Tests

Universal tensile tests were performed on neat PMMA, PMMA/BDBA composites and PMMA/C30B/BDBA nanocomposites. The tensile strength, percentage strain and Young's modulus values of the melt mixed compounds calculated by taking the average of at least three measurements are listed in Table 3.5. Standard deviations were considered in order to analyze the results more preciously. Mechanical results of pure PMMA were slightly lower than the theoretical values because extensometer did not used during the tests. Therefore, the results were only used for comparing the tensile properties of pure PMMA with its composites and nanocomposites.

**Table 3.5.** Tensile tests result of PMMA, PMMA/BDBA and its nanocomposites

| Compounds | wt% BDBA | Young's Modulus (GPa) | Tensile Strength (MPa) | % Elongation at Break |
|---|---|---|---|---|
| **PMMA** | | 1.32 ± 0.09 | 55.50 ± 7.12 | 6.95 ± 0.72 |
| **PMMA/BDBA** | 1 | 1.36 ± 0.09 | 44.03 ± 1.88 | 5.25 ± 0.13 |
| | 3 | 1.34 ± 0.04 | 30.34 ± 5.60 | 4.49 ± 0.44 |
| | 5 | 1.29 ± 0.07 | 26.06 ± 4.20 | 5.46 ± 1.36 |
| | 7 | 1.29 ± 0.20 | 23.64 ± 4.18 | 5.58 ± 1.06 |
| **PMMA/C30B/BDBA** | | 1.35 ± 0.06 | 32.50 ± 3.65 | 4.82 ± 0.30 |
| | 1 | 1.31 ± 0.08 | 36.14 ± 8.08 | 5.00 ± 0.56 |
| | 3 | 1.34 ± 0.08 | 27.76 ± 4.33 | 4.51 ± 0.40 |
| | 5 | 1.22 ± 0.16 | 22.16 ± 7.58 | 5.21 ± 0.62 |
| | 7 | 1.17 ± 0.09 | 21.25 ± 1.46 | 5.11 ± 0.66 |

Apparent Young's modulus values were determined from stress-strain curves of the compounds by applying linear regression analyses. It was found that the effect of boron filler on this property was very small as can be seen in Figure 3.35. As the amount of BDBA incorporated was increased, the modulus value was slightly reduced may be because of the dispersion problem arisen for high boron loadings and/or the decrease in the chain entanglement due to the addition of filler producing the enhanced chain mobility of PMMA. A similar trend was determined for PMMA/C30B/BDBA nanocomposites which shows that boron addition caused a reduction in modulus, up to 1.17 GPa for 7 wt% BDBA.

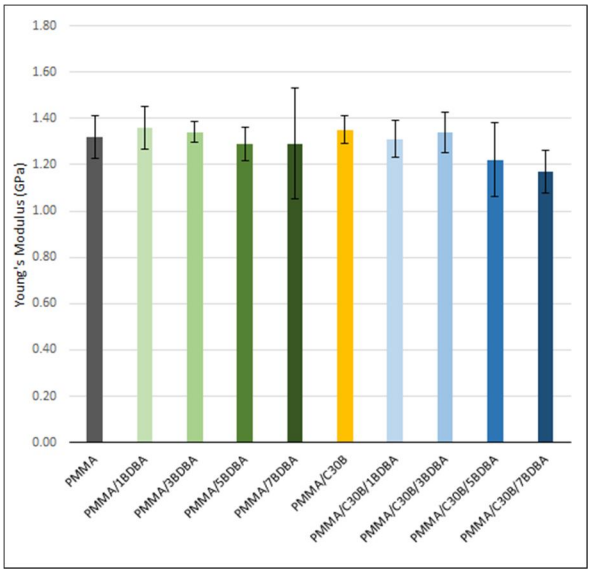


**Figure 3.35.** Apparent Young's modulus of pure PMMA, its composites with BDBA and its nanocomposites with the nanoclay and BDBA obtained by melt mixing.

The effect of boron compound on the tensile strength of PMMA is shown in the Figure 3.36. The tensile strength of pure PMMA measured as 55.5 MPa which was lower than the value reported in the technical data sheet of PMMA. This may be resulted from the processing conditions such as temperature or some

impurities which caused to decrease in mechanical properties of PMMA: When the 1 wt% of BDBA added to the polymer matrix, the tensile strength of the polymer was enormously lowered to 44.0 MPa . Increasing the wt% of BDBA from 1 to 7 showed more reduction in the tensile properties up to 23.6 MPa. It is clear that, addition of boron filler caused a more brittle structure because of agglomeration of boron compound as seen in SEM images of PMMA/BDBA (Figure 3.6 and Figure 3.7). Boronic acids act as stress concentrator sites in the polymer matrix hence higher amount of boron filler caused mechanically weaker products. Addition of the Cloisite 30B did not lead an enhanced in tensile strength because of the same reason as mentioned for boron filler. Even though inclusion of 1 wt% BDBA into PMMA/C30B matrix increased the strength of the composites, the tensile strength value obtained for pure PMMA was not reached any way. 1 wt% of BDBA either in composite or in nanocomposite yielded the best tensile strength values among all the results except for the neat PMMA.

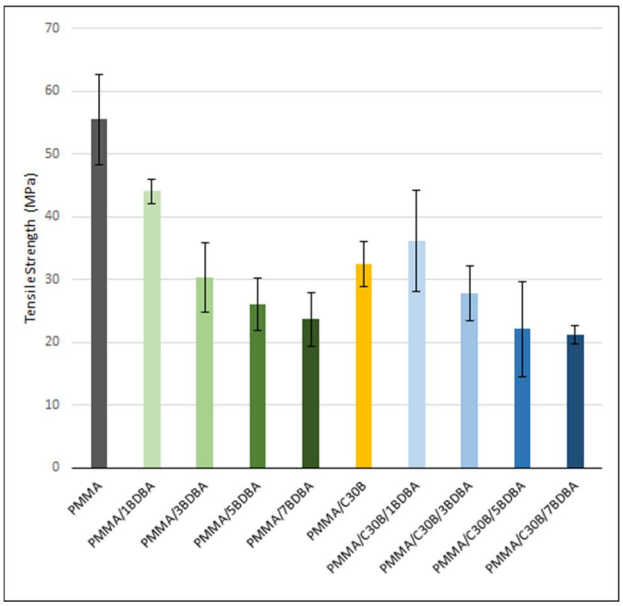


**Figure 3.36.** Tensile strength of pure PMMA, its composites with BDBA and its nanocomposites with the nanoclay and BDBA obtained by melt mixing.

Another important property obtained by tensile test is the elongation of the material at break. Pure PMMA was elongated about 6.95% until fracture occurred. This elongation value was decreased with the addition of boron compound as BDBA caused more brittle structure and stress transfer between BDBA particles and PMMA chains did not exist. However, there is no systematic relation between % elongation and wt% of BDBA incorporated into PMMA matrix as can be seen in Figure 3.37. Higher amount of BDBA enhanced strain property somehow more than those for the lower amounts. The reason of this may be the effect of fillers in chain entanglement of the polymer, existence of higher amount of reinforcements between the polymer chains may create more ductile structures.

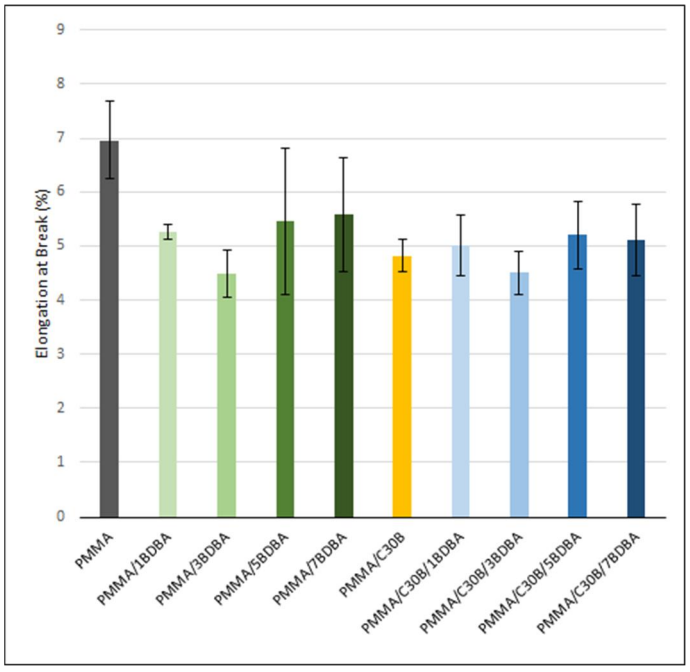


**Figure 3.37.** % Elongation at break of pure PMMA, its composites with BDBA and its nanocomposites with the nanoclay and BDBA obtained by melt mixing.

# CHAPTER 4

# CONCLUSION

In this study, poly(methyl methacrylate), PMMA, composites involving variable amounts of benzene-1,4-diboronic acid, BDBA, were prepared by melt blending and solution casting techniques and their morphologic, thermal, mechanical and flame retardant characteristics were investigated. In addition, organically modified montmorillonite, OMMT, special one Cloisite 30B, C30B, was incorporated into PMMA/BDBA matrices to determine the effects of nanoclay on the properties of the composites.

To study the morphology of the compounds, XRD, TEM and SEM analyses were used. For the solution mixed nanocomposites, the sharp peak of OMMT slightly shifted to lower angles revealing the intercalated structure, on the other hand, for the melt mixed nanocomposites, it totally disappeared pointing out exfoliation of the clay layers. TEM analyses of the nanocomposites indicated intercalated and exfoliated structure for the solution mixed composites whereas mostly intercalated montmorillonite layers for the melt blended analogues. The dispersion of clay layers was not affected by the amount of BDBA filler according to TEM images. SEM images of the composites showed agglomerated boron involving regions for the samples prepared by solution mixing whereas a more homogenous dispersion was observed for the melt blended analogues.

The thermal behaviors of PMMA and its nanocomposites were studied by TGA and DP-MS techniques systematically. TGA analyses demonstrated

improvement in the thermal stability with the addition of the boron and the clay fillers. The maximum rate of degradation temperature, $T_{max}$ was enhanced non-uniformly with the increase in wt% of boron particles. With the addition of 15 wt% BDBA, $T_{max}$ value was improved by 12°C at most. The increase was about 18°C in the presence of OMMT and also formation of a char was seen clearly. No significant difference in thermal behavior was observed for the composites prepared by solution and melt mixing techniques. The solution mixed composites having 15 wt% BDBA displayed an additional high temperature degradation step which can be accepted as an evidence for the presence of a boron network structure decomposing at high temperatures.

DP-MS analyses of compounds indicated that PMMA composites and nanocomposites decomposed via depolymerization mechanism yielding mainly the monomer. The TIC curves shifted to high temperature regions as the amount of boron compound added was increased. In solution mixed PMMA/BDBA composites, the increase in thermal stability of PMMA was associated with the existence of a boron network structure and the trans-esterification reactions between PMMA and BDBA. For the melt mixed composites, the extent of trans-esterification reaction was enhanced, whereas, that of formation of the boron network structure was diminished. It can be concluded that the interaction between PMMA and BDBA are more probable than the interaction between the BDBA particles, for the composites in which distribution of BDBA particles was more homogenous as confirmed by SEM images. In the presence of OMMT, the relative yields of products attributed to the decomposition of the units generated by trans-esterification reaction was increased while those due to the degradation of boron network were almost totally diminished. Thus, it can be concluded that clay layers inhibit accumulation of boron particles and network formation.

Although the dripping behavior of pure PMMA was disappeared for the filled composites and increase in char formation was detected, the flame characteristics of PMMA compounds were not noticeably affected by the addition of neither BDBA nor OMMT. Similarly, only a small amount of improvement, still below 20%, was detected for the LOI values. Limited amount of network structure generated may be the main reason for the very small improvement in LOI values. Therefore, it can be proposed that the amounts of fillers used in this work are not sufficient to produce flame retardant PMMA composites. The tensile strength and % elongation of the composites were decreased in the presence of fillers as expected.

To conclude, the thermal stability of PMMA was noticeably increased upon incorporation of BDBA by both solution and melt mixing techniques. In the presence of OMMT generation of boron net-work structure was almost totally inhibited.

# REFERENCES


[1] Thomas, S., & Zaikov, G. E. (2008). *Polymer nanocomposite research advances*. Nova Publishers.

[2] Nguyen, Q. T., & Baird, D. G. (2006). Preparation of polymer–clay nanocomposites and their properties. *Advances in Polymer Technology*, *25*(4), 270-285.

[3] Olad, A. (2011). Polymer/clay nanocomposites. *Advances in diverse industrial applications of nanocomposites*, 113-138.

[4] Kumar, S., Jog, J. P. and Natarajan, U. (2003), Preparation and characterization of poly(methyl methacrylate)–clay nanocomposites via melt intercalation: The effect of organoclay on the structure and thermal properties. J. Appl. Polym. Sci., 89: 1186–1194. doi: 10.1002/app.12050

[5] Kumar, M., Arun, S., & Upadhyaya, P. (2015). Properties of PMMA/Clay Nanocomposites prepared using different compatibilizers. International Journal of Mechanical and Materials Engineering, 10(7). doi:10.1186/s40712-015-0035-x

[6] Maurizio G. (2012). Rubber Clay Nanocomposites, Advanced Elastomers - Technology, Properties and Applications, D.Sc. Anna Boczkowska (Ed.), ISBN: 978-953-51-0739-2, InTech, DOI: 10.5772/51410. Available from: http://www.intechopen.com/books/advanced-elastomers-technology-properties-and-applications/rubber-clay-nanocomposites

[7] Vaia, R. A., Ishii, H., & Giannelis, E. P. (1993). Synthesis and properties of two-dimensional nanostructures by direct intercalation of polymer melts in layered silicates. Chemistry of Materials, 5(12), 1694-1696.

[8] Aranda, P., & Ruiz-Hitzky, E. (1992). Poly (ethylene oxide)-silicate intercalation materials. Chemistry of Materials, 4(6), 1395-1403.

[9] Fu, J. & Naguib, H. E. (2006). Effect of nanoclay on the mechanical properties of PMMA/clay nanocomposite foams. Journal of cellular plastics, 42(4), 325-342.

[10] Sato, H., Ohtani, H., Harada, R., Tsuge, S., Kato, M., & Usuki, A. (2006). Polymer/silicate Interaction in Nylon 6-Clay Hybrid Studied by Temperature Programmed Pyrolysis Techniques. Polymer Journal, 38, 171-177. Retrieved February 12, 2016, from http://www.nature.com/pj/journal/v38/n2/abs/pj200623a.html

[11] Wilkie, C. A., & Morgan, A. B. (Eds.). (2009). Fire retardancy of polymeric materials. CRC Press.

[12] Doğan, M., PhD. (2011). Production and Characterization of Boron Containing Flame Retardant Polyamide-6 and Polypropylene Composites and Fibers (Unpublished doctoral dissertation). Middle East Technical University. Retrieved February 16, 2016, from https://etd.lib.metu.edu.tr/upload/12613266/index.pdf

[13] İbibikcan, E., Ms. (2013). Use of Boron Compounds as Synergistic Flame Retardant in Low Density Polyethylene – Ethylene Vinyl Acetate Blends and Nanocomposites (Unpublished master's dissertation). Middle East Technical University. Retrieved February 16, 2016, from http://etd.lib.metu.edu.tr/upload/12616024/index.pdf

[14] Ayrilmis, N., Akbulut, T., Dundar, T., White, R. H., Mengeloglu, F., Buyuksari, U.,& Avci, E. (2012). Effect of boron and phosphate compounds on physical, mechanical, and fire properties of wood–polypropylene composites. Construction and Building Materials, 33, 63-69.

[15] Morgan, A. B., Jurs, J. L., & Tour, J. M. (2000). Synthesis, flame-retardancy testing, and preliminary mechanism studies of nonhalogenated aromatic boronic acids: A new class of condensed-phase polymer flame-retardant additives for acrylonitrile–butadiene–styrene and polycarbonate. Journal of applied polymer science, 76(8), 1257-1268.

[16] Hall, D. G. (2005). Boronic Acids: Preparation, applications in organic synthesis and medicine. Retrieved February 16, 2016, from https://books.google.com.tr/books?hl=tr&lr=&id=alB2z5OZPZ4C&oi=fnd&pg=PA1&dq=transesterification of boronic acid&ots=SBf5YF3Qsl&sig=62WetkWlVsOX7J0qGVowcDtG-Iw&redir_esc=y#v=onepage&q=transesterification of boronic acid&f=false.

[17] Štefková, P. (2006). Measurement of Thermophysical Properties of PMMA by Pulse Transient Method. Retrieved February 7, 2016, from http://www.fch.vutbr.cz/stc/download/DSP2006/Stefkova_2006.pdf

[18] "The ACRYLITE® brand – ACRYLITE® – Colors, patterns and functions". Retrieved February 06, 2016 from http://www.acrylite.net/product/acrylite/en/about/acrylite-brand/pages/default.aspx

[19] "Trademark Electronic Search System". TESS. US Patent and Trademark Office. p. Search for Registration Number 0350093. Retrieved February 06, 2016

[20] Charles A. Harper; Edward M. Petrie (10 October 2003). Plastics Materials and Processes: A Concise Encyclopedia. John Wiley & Sons. p. 9. ISBN 978-0-471-45920-0.

[21] Balke, S. T. (1972). The free radical polymerization of methyl methacrylate to high conversions (Doctoral dissertation, McMaster University).

[22] Teng, H., Koike, K., Zhou, D., Satoh, Z., Koike, Y. and Okamoto, Y. (2009), High glass transition temperatures of poly(methyl methacrylate) prepared by free radical initiators. J. Polym. Sci. A Polym. Chem., 47: 315–317. doi:10.1002/pola.23154

[23] Harper, C. A., & Petrie, E. M. (2003). Plastics materials and processes: A concise encyclopedia. Retrieved February 06, 2016, from

https://books.google.com.tr/books?id=oe5YJmRmxQMC&pg=PA9&redir_esc=y#v=onepage&q&f=false

[24] Feldman, D. (1991), Properties of polymers, 3rd edition, by D. W. van Krevelen, Elsevier Science Publishers, Amsterdam, Oxford, New York, 1990,875 pages, US$337.25. J. Polym. Sci. B Polym. Phys., 29: 1654. doi:10.1002/polb.1991.090291313

[25] Poly(methyl-methacrylate) (PMMA). (n.d.). Retrieved February 07, 2016, from http://steinwall.com/pages/Poly(methyl-methacrylate)(PMMA)/

[26] Manring, L. E. (1991). Thermal degradation of poly(methyl methacrylate). 4. Random side-group scission. Macromolecules, 24(11), 3304-3309.

[27] Kashiwagi, T., Inaba, A., Brown, J. E., Hatada, K., Kitayama, T., & Masuda, E. (1986). Effects of weak linkages on the thermal and oxidative degradation of poly (methyl methacrylates). Macromolecules, 19(8), 2160-2168.

[28] Song, J., Fischer Ch.H. and Schnabel, W. (1992). Thermal Oxidative Degradation of Poly(methyl methacrylate), Polymer Degradation and Stability, 36: 261–266.

[29] Zeng, W. R., Li, S. F., & Chow, W. K. (2002). Review on Chemical Reactions of Burning Poly(methyl methacrylate) PMMA. Journal of Fire Sciences, 20(5), 401-433.

[30] Motaung, T. E., Luyt, A. S., Saladino, M. L., Martino, D. C., & Caponetti, E. (2012). Morphology, mechanical properties and thermal degradation kinetics of PMMA-zirconia nanocomposites prepared by melt compounding. Polym Lett,6(11), 871-881.

[31] Elimat, Z. M., Zihlif, A. M., & Avella, M. (2008). Thermal and optical properties of poly(methyl methacrylate)/calcium carbonate nanocomposite. Journal of Experimental Nanoscience, 3(4), 259-269.

[32] Philip, B., Abraham, J. K., Chandrasekhar, A., & Varadan, V. K. (2003). Carbon nanotube/PMMA composite thin films for gas-sensing applications. Smart materials and structures, 12(6), 935.

[33] Boudjema, S., & Djellouli, B. (2014). Characterization of Organomontmorillonite (Organo-MMT) and Study of Its Effects Upon the Formation of Poly(methyl methacrylate)/Organo-MMT Nanocomposites Prepared by in Situ Solution Polymerization. Russian Journal of Applied Chemistry, 87(10), 1464−1473-1464−1473. doi:10.1134/S1070427214100127

[34] Di Pasquale, G., & Pollicino, A. (2015). PMMA/o-MMT nanocomposites obtained using thermally stable surfactants. Journal of Applied Polymer Science, 132, 41393, doi: 10.1002/app.41393.

[35] Pandey, P., Dayanidhi, A., Mohanty, S., & Nayak, S. (2011). Effect of clay loading on flammability of poly(methyl methacrylate)/clay nanocomposites. Journal of Thermoplastic Composite Materials, 26(5), 663–679-663–679. doi:10.1177/0892705711428655

[36] Chang, K. C., Chen, S. T., Lin, H. F., Lin, C. Y., Huang, H. H., Yeh, J. M., & Yu, Y. H. (2008). Effect of clay on the corrosion protection efficiency of PMMA/$Na^{+}$-MMT clay nanocomposite coatings evaluated by electrochemical measurements. European Polymer Journal, 44(1), 13-23.

[37] Cui, Y., Kumar, S., Kona, B. R., & van Houcke, D. (2015). Gas barrier properties of polymer/clay nanocomposites. RSC Advances, 5(78), 63669-63690.

[38] Unnikrishnan, L., Mohanty, S., & Nayak, S. K. (2014). Evaluation of flame retardancy and shear resistivity characteristics of organoclay within acrylate polymer. Journal of Thermal Analysis and Calorimetry, 118(1), 405-416.

[39] Lerari, D., Peeterbroeck, S., Benali, S., Benaboura, A., & Dubois, P. (2011). Combining atom transfer radical polymerization and melt compounding for producing PMMA/clay nanocomposites. Journal of Applied Polymer Science, 121(3), 1355-1364.

[40] Huang, G., Guo, H., Yang, J., Wang, X., & Gao, J. (2013). Effect of the Phosphorus–Nitrogen-Containing Quaternary Ammonium Salt Structure

on the Flammability Properties of Poly(methyl methacrylate)/Montmorillonite Nanocomposites. Industrial & Engineering Chemistry Research Ind. Eng. Chem. Res., 52(11), 4089-4097.

[41] Kim, S., & Wilkie, C. A. (2008). Transparent and flame retardant PMMA nanocomposites. Polymers for Advanced Technologies, 19(6), 496-506.

[42] Kiran, M. S. R. N., Raidongia, K., Ramamurty, U., & Rao, C. N. R. (2011). Improved mechanical properties of polymer nanocomposites incorporating graphene-like BN: Dependence on the number of BN layers. Scripta Materialia,64(6), 592-595.

[43] Koysuren O., Karaman M., Yıldız H.B., Koysuren H.N.& Dinc H. (2014) Electrospun Polyvinyl Borate/Poly(methyl methacrylate) (PVB/PMMA) Blend Nanofibers, International Journal of Polymeric Materials and Polymeric Biomaterials, 63:7, 337-341, DOI: 10.1080/00914037.2013.845188

[44] Doğan, M., Alkan, M., Turhan, Y., Gündüz, Z., Beyli, P., & Doğan, S. (2015). Synthesis, Characterization and Rheological Properties of Boronoxide, Polymer Nanocomposites. Retrieved April 11, 2016, from http://waset.org/pdf/books/?id=21154&pageNumber=535

[45] Yuan, Y., Zhang, L., Hu, L., Wang, W., & Min, G. (2011). Size effect of added $LaB_6$ particles on optical properties of $LaB_6$ /polymer composites. Journal of Solid State Chemistry, 184(12), 3364-3367.

[46] Özgen, C. (2012). The Characterization of Some Methacrylate and Acrylate Homopolymers, Copolymers and Fibers Via Direct Pyrolysis Mass Spectroscopy (Unpublished doctoral dissertation) Middle East Technical University. Retrieved June 17, 2015, from http://etd.lib.metu.edu.tr/upload/12615308/index.pdf